Reactivity of Alkynes toward M–η^2-CS_2 Metal Complexes. 3. The Coupling Products Obtainable with Bis(cyclopentadienyl)molybdenum Fragments and Their Relative Stability

Françoise Conan,[1] Jean Sala-Pala,[1] Jacques E. Guerchais,*[,1] Jing Li,[2] Roald Hoffmann,*[,2] Carlo Mealli,*[,3] René Mercier,[4] and Loïc Toupet[5]

UA CNRS 322 Université de Bretagne Occidentale, 29287 Brest Cedex, France, Department of Chemistry, Cornell University, Ithaca, New York 14853, the Istituto de Stereochimica ed Energetica dei Composti di Coordinazione, CNR-Via J. Nardi 39, 50132 Florence, Italy, UA CNRS 436, Université de Franche-Comté, 25030, Besançon Cédex, France, and UA CNRS 804, Université de Rennes, 35042 Rennes-Cédex, France

Received November 22, 1988

[Cp_2Mo–η^2-CS_2] (**1**) is shown to react with one, two, and three molecules of activated alkynes. The nature of the different coupling products and the reaction conditions are described. In particular, while $CF_3C{\equiv}CCF_3$ reacts with **1** to give the metallacycle derivative [$Cp_2\overline{MoC(S)SC(R){=}C(R)}$] (**2**, R = CF_3), the reaction of **1** with $CO_2MeC{\equiv}CCO_2Me$ affords two isomers: **3**, the analogue of **2** with R = CO_2Me, and [$Cp_2\overline{MoSC(S)C(R){=}CR}$] (**4**, R = CO_2Me). The complexes obtained from the reaction of HC≡CCN with **2** and **3**, [$Cp\overline{Mo\{C_5H_4C(SCH{=}CHCN)SC(R){=}CR\}}$] (**5**, R = CF_3; **6**, R = CO_2Me), correspond to a new type of combination of CS_2 with two alkynes. Direct reaction of **1** with HC≡CCN does not yield an analogue of complexes **5** and **6** but gives depending on the experimental conditions either compound **7** [$Cp_2Mo(C_{10}H_3N_3S_2)$], the first example of a complex in which CS_2 is combined with three molecules of alkyne, or [$Cp_2Mo(\eta^2$-$CS_3)$] (**8**) and [S((*Z*)-CH=CHCN)$_2$] (**9**). The crystal and molecular structures of complexes **2**, **4**, **6**, and **7** have been determined by single-crystal X-ray diffraction studies. **2** crystallizes in the monoclinic space group $P2_1/c$ with a = 13.032 (2) Å, b = 8.066 (2) Å, c = 18.155 (2) Å, β = 124.70 (1)°, U = 1569 (1) Å^3, and Z = 4. **4** crystallizes in the triclinic space group $P\bar{1}$ with a = 7.662 (4) Å, b = 14.661 (5) Å, c = 15.414 (4) Å, α = 96.00 (3)°, β = 96.19 (3)°, γ = 90.79 (4)°, U = 1711.3 (5) Å^3, and Z = 4. **6** crystallizes in the monoclinic space group $P2_1/c$ with a = 10.246 (4) Å, b = 15.245 (9) Å, c = 15.140 (8) Å, β = 103.89 (5)°, U = 2296 (2) Å^3, and Z = 4. **7** crystallizes in the orthorhombic space group *Pbca* with a = 22.089 (5) Å, b = 10.699 (2) Å, c = 15.660 (3) Å, U = 3701 (2) Å^3, and Z = 8. Extended Hückel calculations and qualitative MO theory are used to analyze the electronic features of the most simple models obtainable from the coupling of CS_2 with an alkyne molecule, namely, $Cp_2\overline{MoC(S)SC(R){=}C(R)}$ (complexes **2** and **3**) and $Cp_2\overline{MoSC(S)C(R){=}C(R)}$ (complex **4**). The study illustrates the major orbital effects and points out that in the course of the coupling reaction to form the latter complex, the metal may undergo an oxidation state change.

Introduction

In two preceding papers,[6,7] some of us have investigated the reactivity of complexes of the type L_4M–η^2-CS_2 with activated alkynes {L_4M = (triphos)ClRh or $(CO)_2(PR_3)_2Fe$ [triphos = $CH_3(CH_2PPh_2)_3$]}. It is now clear that the heteroallene in the η^2-coordination mode becomes a polyfunctional reaction center, basically nucleophilic at the exocyclic sulfur atom (S_{exo}) and electrophilic at the carbon atom. Moreover, upon geometrical rearrangement also the metal and the originally coordinated sulfur atom (S_{endo}) may become susceptible to attack.[8] Alternative reaction pathways may be taken depending on the nature (electronegativity) of the substituents, either on the metal fragment and/or on the attacking alkyne (Figure 1). Experimentally it has been shown that by opportunely selecting the donor strength of the phosphine ligands in $(CO)_2(PR_3)_2Fe$, two different types of rings (A and B, see Figure 1) both incorporating CS_2 may be produced.[10] In one case the rings interconvert with each other, thus establishing an equilibrium. In the case of the rhodium species two alkyne molecules are taken up by the system, giving rise to a complex metallacyclobutene compound, probably in two successive steps.[6]

The isolobal analogy[15] is often applied successfully to compare complex molecules of apparently very different nature and to find a rationale for their similar chemical behavior. The d^8 ML_4 and the d^4 MCp_2 fragments represent a good example of the analogy at work. Of interest to us is the comparable capability of these fragments to stabilize η^2 coordination of carbon disulfide, with evident similarities in the geometry of the two inner M–η^2-CS_2

(1) Université de Bretagne Occidentale.
(2) Cornell University.
(3) ISSECC, CNR.
(4) Université de Franche-Comté.
(5) Université de Rennes.
(6) Bianchini, C.; Mealli, C.; Meli, A.; Sabat, M.; Silvestre, J.; Hoffmann, R. *Organometallics* **1986**, *5*, 1733.
(7) Li, J.; Hoffmann, R.; Mealli, C. *Organometallics* preceding paper in this issue.
(8) Bianchini, C.; Mealli, C.; Meli, A.; Sabat, M. *Stereochemistry of Organometallic and Inorganic Compounds*, Bernal, I., Ed.; Elsevier: Amsterdam, 1986; Vol. 1, pp 146–254.
(9) Le Marouille, J. Y.; Lelay, C.; Benoit, A.; Grandjean, D.; Touchard, D.; Le Bozec, H.; Dixneuf, P. H. *J. Organomet. Chem.* **1980**, *191*, 133.
(10) Le Bozec, H.; Gorgues, A.; Dixneuf, P. H. *Inorg. Chem.* **1981**, *20*, 2486.
(11) Frazier, C. C.; Magnussen, N. D.; Osuji, L. N.; Parker, K. O. *Organometallics* **1982**, *1*, 903.
(12) (a) Schenk, W. A.; Schwietzke, T.; Müller, H. *J. Organomet. Chem.* **1982**, *232*, C41. (b) Schenk, W. A.; Kuemmerle, D.; Burschka, C. *J. Organomet. Chem.* **1988**, *349*, 163.
(13) Bianchini, C.; Meli, A.; Scapacci, G. *Organometallics* **1985**, *4*, 264.
(14) Wakatsuki, Y.; Yamazaki, H.; Iwasaki, H. *J. Am. Chem. Soc.* **1973**, *95*, 5781.
(15) Hoffmann, R. *Angew. Chem., Int. Ed. Engl.* **1982**, *21*, 711.

0276-7333/89/2308-1929$01.50/0

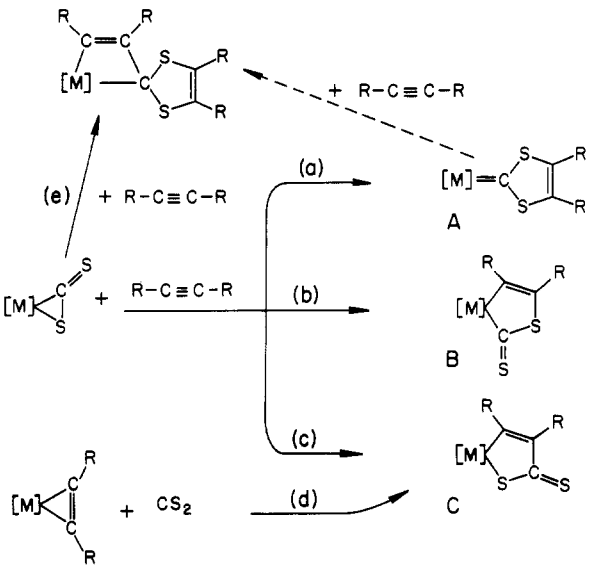

Figure 1. Addition reactions between alkynes and $[M(\eta^2\text{-}CS_2)]$ complexes and related reactions: (a) [M] = $[CpMn(CO)L]$,[9] $[Fe(CO)_2L_2]$,[10] $[Cr(\eta^6\text{-arene})(CO)_2]$,[11] $[W(CO)_3(R_2PCH_2CH_2PR_2)]$,[12] and [Ni(triphos)][13] (only the structure of the Mn derivative has been confirmed by a X-ray study);[9] (b) [M] = $[CpRh(PPh_3)]$,[14] $[Fe(CO)_2L_2]$[10] (no X-ray data available for type B complexes; in this work [M] = $[Cp_2Mo]$ with R = CF_3 (**2** with X-ray crystal structure) and R = CO_2Me (**3**)); (c and d) no type C complex previously reported from reaction c, but only from reaction d with [M] = $[CpM(PPh_3)]$ (M = Co, Rh) (no X-ray data available)[14] (in this work, reaction c with [M] = $[Cp_2Mo]$ and R = CO_2Me (**4** with X-ray crystal study); (e) [M] = [Rh(triphos)Cl][8] (this is the only example of a 2:1 addition of an alkyne to an η^2-CS_2 complex; the 1:1 type A adduct should be an intermediate in this reaction).

groupings. The gross geometric features alone are not always able to control the reactivity pattern. Subtle factors, other than the primary coordination, can redirect the evolution of the chemical species.

In this paper we present in detail the different chemical reactions of activated alkynes with $(Cp)_2Mo\text{-}\eta^2\text{-}CS_2$ and the characterization of the resulting products. A brief summary of part of this experimental work has already appeared.[16] Up to three molecules of alkyne can be taken up by the system, whose complexity in this case prevents any serious attempt to describe the mechanism of the formation reaction. Accordingly the theoretical analysis presented in the final section of the paper is limited to the least intricate CS_2–C_2H_2 coupling reactions. In particular we will focus on the role of the precursor complex $(Cp)_2Mo\text{-}\eta^2\text{-}CS_2$ and we will try to underline similarities and differences with the previously treated iron species $(PR_3)_2(CO)_2Fe\text{-}\eta^2\text{-}CS_2$.[10]

Experimental Section

1. General Procedures and Physical Measurements. All reactions were performed in Schlenk tubes in a dry oxygen-free dinitrogen atmosphere. All solvents were distilled by standard techniques and thoroughly deoxygenated before use. All elemental analyses were performed by "Centre d'Analyse du CNRS". The mass spectra were obtained with a Varian MAT 311 spectrophotometer. The IR spectra were measured on a Perkin-Elmer 1430 spectrometer. ^1H, ^{13}C, and ^{19}F NMR spectra were recorded by using JEOL FX100 and Brucker AC300 and AM400 spectrometers operating in the FT mode. For ^1H and ^{13}C NMR spectra, TMS was used as internal reference while for ^{19}F NMR spectra CF_3CO_2H was used as an external reference. Unless otherwise stated, NMR data have been obtained by using $CDCl_3$ as solvent.

$[Mo(\eta^5\text{-}C_5H_5)_2(\eta^2\text{-}CS_2)]$ (1) and HC≡CCN were prepared as previously described.[17]

2. Reaction between 1 and $CF_3C{\equiv}CCF_3$: Access to Complex (2). An excess of $CF_3C{\equiv}CCF_3$ was added at ca. −120 °C to a THF solution of **1**. After being warmed to room temperature, the solution was stirred for ca. 12 h. The solvent was removed under reduced pressure and the residue extracted with dichloromethane. After filtration, the resulting solution was chromatographed on a silica gel column made up with hexane. Elution with hexane gave an orange-brown phase that could not be identified. Elution with a 1:1 dichloromethane–hexane mixture gave a dark green powder, the recrystallization of which in dichloromethane and hexane afforded **2** as dark green crystals in ca. 30% yield. Anal. Calcd for $C_{15}H_{10}F_6S_2Mo$: C, 38.8; H, 2.1; S, 13.8; Mo, 20.7. Found: C, 39.0; H, 2.1; S, 12.7; Mo, 21.6. Mass: parent peak P^+ observed at m/e 465.9182 (calcd 465.9182 with ^{98}Mo). ^1H NMR (99.6 MHz, δ): 5.11 (10, s), Cp. ^{19}F NMR (99.6 MHz, δ): 22.7 (3, qu, $^5J_{FF}$ = 14.7 Hz), CF_3; 31.3 (3, qu, $^5J_{FF}$ = 14.7 Hz) CF_3. ^{13}C NMR[18] (100.2 MHz, δ): 93.9 (s), Cp; 118.5, (qu, $^1J_{CF}$ = 281 Hz) and 127.2 (qu, $^1J_{CF}$ = 276 Hz), C(4) and C(5); 153.0 (qu qu, $^2J_{CF}$ = 31 Hz, $^3J_{CF}$ = 6 Hz) and 156.5 (qu qu, $^2J_{CF}$ = 31 Hz, $^3J_{CF}$ = 2 Hz), C(2) and C(3); 310.3 (s), C(1).

3. Reaction of 1 with $CO_2MeC{\equiv}CCO_2Me$ (dmad): Access to Complexes 3 and 4. To a THF solution of **1** (2.3 mmol) was added a THF solution of dmad (2.1 mmol). After reflux (ca. 5 h), the solvent was removed under reduced pressure; then the residue was extracted with dichloromethane and the resulting solution chromatographed on a silica gel column made up with a 1:1 dichloromethane–hexane mixture. Elution with dichloromethane gave an orange-brown phase which after evaporation to dryness and recrystallization (dichloromethane and hexane) afforded **3** as an orange-brown microcrystalline powder in ca. 30% yield. Further elution with a 4:1 dichloromethane–THF mixture gave a phase which after recrystallization (dichloromethane–hexane) afforded **4** as dark green crystals in ca. 20% yield. Anal. Calcd for $C_{17}H_{16}O_4S_2Mo{\cdot}0.25CH_2Cl_2$ (**3**): C, 44.5; H, 3.5; Cl, 3.8. Found: C, 44.3; H, 3.4; Cl, 3.6. Mass: parent peak P^+ found at m/e 445.9556 (calcd 445.9540 with ^{98}Mo). ^1H NMR (99.6 MHz, δ): 3.76 (3, s), CH_3; 3.80 (3, s), CH_3; 5.10 (10, s), Cp; 5.36 (s, 0.5), CH_2Cl_2. ^{13}C NMR[18] (100.2 MHz, δ): 51.6 and 52.3, C(15) and C(17); 93.5, Cp; 148.8 and 158.8, C(12) and C(13); 174.7 and 177.4, C(14) and C(16); 313.1, C(11). Anal. Calcd for $C_{17}H_{16}O_4S_2Mo$ (**4**): C, 45.9; H, 3.6; S, 14.4; Mo, 21.6. Found: C, 45.8, H, 3.5; S, 13.9; Mo, 20.7. Mass: parent peak P^+ observed at m/e 445.9550 [calcd 445.9540 with ^{98}Mo]. ^1H NMR (99.6 MHz, δ): 3.76 (3, s), CH_3; 3.78 (3, s), CH_3; 5.24 (10, s), Cp. ^{13}C NMR[18] (100.2 MHz, δ): 51.7 and 52.2, C(15) and C(17); 93.3, Cp; 161.0 and 167.2, C(12) and C(13); 176.9 and 178.4, C(14) and C(16); 246.7, C(11).

4. Reaction of HC≡CCN with Complexes 2 and 3: Access to Complexes 5 and 6. **5** and **6** are prepared from **2** and **3**, respectively, by procedures similar to those described here for **5**. A dichloromethane solution containing **2** (2 mmol) and a large excess of HC≡CCN (ca. 10 mmol) was stirred for ca. 24 h, at room temperature. After concentration under reduced pressure, the solution was chromatographed on a silica gel column made up with hexane. Elution with a 1:1 dichloromethane–hexane mixture gave small amounts of an unidentified product. Elution with dichloromethane gave after recrystallization (dichloromethane–hexane) as red-orange microcrystals in ca. 55% yield (similar yield for the dark red complex **6** starting from **3**. Anal. Calcd for $C_{18}H_{11}F_6NS_2Mo$ (**5**): C, 41.9; H, 2.1; F, 22.1; N, 2.7; Mo, 18.6. Found: C, 42.0; H, 2.3; F, 22.3; N, 2.6; Mo, 18.3. ^1H NMR[18] (300.1 MHz, δ): 4.16 (1, m), 5.01 (2, m), 6.20 (1, m), ABB'C system C_5H_4; 5.22 (5, s), Cp; 5.24 (1, d, $^3J_{HH}$ = 10.2 Hz), HC(13); 7.36 (1, d, $^3J_{HH}$ = 10.2 Hz), HC(12). ^{19}F NMR (99.6 MHz, δ): 20.6 (3, qu, $^5J_{FF}$

(16) Conan, F.; Guerchais, J. E.; Mercier, R.; Sala-Pala, J.; Toupet, L. *J. Chem. Soc., Chem. Commun.* **1988**, 345.

(17) (a) Okuda, J. Dissertation, Technische Hochschule Aachen, 1984. (b) Okuda, J.; Herberich, G. E. *J. Organomet. Chem.* **1987**, *320*, C35. (c) Moureu, C.; Bongrand, J. C. *Ann. Chim.* **1920**, *14*, 6.

(18) For **2**, **4**, **6**, and **7**, assignment of the NMR signals refers to the numbering schemes used in the X-ray studies (Figures 3–7). For **3**, labeling scheme identical with that given for **4** except permutation of S(2) and C(11) positions (Figure 5). For **5**, labeling scheme similar to that of **6** for the framework (Figure 6).

Table I. Crystallographic Data for the Structural Analyses for Compounds 2, 4, 6, and 7

	2	4	6	7
		A. Crystal Data		
formula	$C_{15}F_6H_{10}MoS_2$	$C_{17}H_{16}MoO_4S_2$	$C_{20}H_{17}MoNO_4S_2CH_2Cl_2$	$C_{20}H_{13}MoN_3S_2$
mol wt	464.30	444.38	580.36	455.41
cryst system	monoclinic	triclinic	monoclinic	orthorhombic
space group	$P2_1/c$	$P\bar{1}$	$P2_1/c$	$Pbca$
a, Å	13.032 (2)	7.662 (4)	10.246 (4)	22.089 (5)
b, Å	8.066 (2)	14.661 (5)	15.245 (9)	10.699 (2)
c, Å	18.155 (2)	15.414 (4)	15.140 (8)	15.660 (3)
α, deg		96.00 (3)		
β, deg	124.70 (1)	96.19 (3)	103.89 (5)	
γ, deg		90.79 (4)		
U, Å^3	1569 (1)	1711.3 (5)	2296 (2)	3701 (2)
Z	4	4	4	8
D_{calcd}, g·cm^{-3}	1.97	1.73	1.68	1.64
μ(Mo Kα), cm^{-1}	10.44	9.99	9.90	9.00
		B. Data Collection and Reduction		
cryst size, mm	0.30 × 0.20 × 0.20	0.20 × 0.25 × 0.25	0.22 × 0.23 × 0.23	0.40 × 0.08 × 0.03
diffractometer		Enraf-Nonius CAD-4		
radiation (λ, Å)		graphite-monochromated Mo Kα (0.71069)		
scan method	ω–2θ	ω–2θ	ω–2θ	ω–2θ
2θ range, deg	≤64	≤54	≤55	≤56
data measd	5750	6260	4373	4072
obsd data	3247 [$I \geq 4\sigma(I)$]	5030 [$I \geq 4\sigma(I)$]	3019 [$I \geq \sigma(I)$]	1247 [$I \geq 4\sigma(I)$]
		C. Solution and Refinement		
no. of variables	142	530	332	120
R	0.052	0.038	0.041	0.059
R_w	0.054	0.032	0.039	0.052
final diff map elec density, e·Å^{-3}	1.28[a]	0.35	0.30	1.15

[a] These positive peaks correspond to the hydrogen atoms of the cyclopentadienyl rings which have not been included in the refinement.

= 14.2 Hz), CF_3; 33.3 (3, qu, $^5J_{FF}$ = 14.2 Hz), CF_3. ^{13}C NMR[18] (75.4 MHz, δ): 77.4, 86.9, 88.5, 92.0, C(6) ···C(9); 92.2, Cp; 101.8, C(10); 118.1 (qu, $^1J_{CF}$ = 279 Hz) and 125.9 (qu, $^1J_{CF}$ = 274 Hz), C(17) and C(19); 116.6 and 155.1, C(13) and C(12); 115.4, C(14). IR (KBr, cm^{-1}): 2200 (m, ν(CN)). Anal. Calcd for $C_{20}H_{17}NO_4S_2Mo{\cdot}CH_2Cl_2$ (**6**): C, 43.5; H, 3.3; N, 2.4; S, 11.0. Found: C, 44.5; H, 3.4; N, 2.2; S, 11.3. ^1H NMR[18] (300.1 MHz, δ): 4.22 (1, m), 4.80 (1, m), 5.11 (1, m), 6.09 (1, m), ABCD system C_5H_4; 5.18 (5, s), Cp; 5.20 (1, d, $^3J_{HH}$ = 10.4 Hz), HC(13); 7.42 (1, d, $^3J_{HH}$ = 10.4 Hz), HC(12); 3.63 (1, s) and 3.65 (1, s), OCH_3. ^{13}C NMR[18] (75.4 MHz, δ): 51.2 and 52.2, C(18) and C(20); 86.6, 87.6, 91.1, 92.6, C(6)···(9); 92.0, Cp; 102.7, C(10); 115.8, C(13); 141.2 and 158.6, C(15) and C(16); 155.7, C(12); 166.7 and 175.5, C(17) and C(19). IR (KBr, cm^{-1}): 2200 (m) (ν(CN)).

5. Reaction of 1 with HC≡CCN: Access to Compounds 7, 8, and 9. Synthesis of 7. A THF solution containing **1** (2.5 mmol) and HC≡CCN (ca. 10 mmol) was stirred at room temperature for ca. 40 h. The solvent was then removed under reduced pressure and the brown-dark residue extracted with dichloromethane. After filtration on Celite, the filtrate was concentrated and chromatographed on a silica gel column made up with hexane. Elution with a 2:1 dichloromethane–hexane gave very small amounts of **9** (see below); then elution with pure dichloromethane afforded, after concentration and recrystallization (dichloromethane–hexane), **7** as orange needles in ca. 16% yield. Anal. Calcd for $C_{20}H_{13}N_3S_2Mo$ (**7**): C, 52.8; H, 2.9; N, 9.2; S, 14.1; Mo, 21.1. Found: C, 52.5; H, 2.8; N, 9.8; S, 14.5; Mo, 20.8. Mass: parent peak P^+ observed at m/e 456.9698 (calcd 456.9731 with ^{98}Mo). ^1H NMR[18] (300.1 MHz, CD_2Cl_2, δ): 4.03 (1, s), HC(22); 5.24 (5, s), Cp; 5.27 (5, s), Cp; 5.41 (1, d, $^3J_{HH}$ = 10.2 Hz), HC(12); 7.62 (1, d, $^3J_{HH}$ = 10.2 Hz), HC(11). ^{13}C NMR[18] (75.4 MHz, CD_2Cl_2, δ): 32.8, C(22); 95.3, Cp; 95.4, Cp; 116.1, 116.5, 118.5, C(13), C(23), C(33); 184.5, C(1). IR (CH_2Cl_2, cm^{-1}): 2240 (w), 2210 (m), 2180 (s) (ν(CN)).

Access to 8 and 9. A similar procedure to that described for **7** was followed starting from a dichloromethane solution containing **1** (2.8 mmol) and HC≡CCN (ca. 3 mmol) (−20 °C for ca. 4 h). Elution with a 2:1 dichloromethane–hexane mixture gave **9**. After sublimation (10^{-2} mmHg, 100 °C), **9** appeared as colorless needles [yield ca. 3%]. Elution with dichloromethane gave, after concentration and recrystallization (dichloromethane–hexane), **8** as brown-orange microcrystals (yield ca. 20%). Anal. Calcd for $C_{11}H_{10}S_3Mo$ (**8**): C, 39.5; H, 3.0; S, 28.7; Mo, 28.7. Found: C, 39.3, H, 3.0; S, 28.9; Mo, 29.6. Mass: parent peak P^+ observed at m/e 336 (calcd 336 with ^{98}Mo). ^1H NMR (300.1 MHz, CD_2Cl_2, δ): 5.25, s, Cp. IR (KBr, cm^{-1}): 1010 (vs br) (νC=S)); 865 (m) (ν(C—S)); no ν(CN) absorption detected. Anal. Calcd for $C_6H_4N_2S$ (**9**): C, 52.9; H, 2.9; N, 20.6. Found: C, 52.7; H, 3.0, N, 20.4. Mass: parent peak P^+ observed at m/e 136 (calcd 136). ^1H NMR (99.6 MHz, δ): 5.60 (2, d, $^3J_{HH}$ = 10.2 Hz), HCCN; 7.25 (2, d, $^3J_{HH}$ = 10.2 Hz), HCS. IR (CH_2Cl_2, cm^{-1}): 2216 (s) (ν(CN)).

6. Crystal Structure Determinations. Crystal data, data collection parameters, and results of the analyses are given in Table I. All measurements were done at 20 °C. Unit-cell dimensions were obtained by least-squares methods from setting angles of 25 randomly selected reflections. During data collection, the intensity of a standard reflection was checked periodically, giving a reference to put the reflection data file on a common scale; no significant variation of this standard was observed throughout each data collection. Only Lorentz and polarization corrections were applied, the absorption correction being too small to be efficient. Neutral atom scattering factors for all non-hydrogen atoms with anomalous dispersion terms were taken from ref 19.

All the structures were solved by a combination of Patterson and difference Fourier techniques and refined by the full-matrix least-square methods with the SHELX-76 package of programs.[20] All non-hydrogen atoms were refined by using anisotropic thermal parameters for **4** and **6** while the carbon atoms of **2** and the carbon and nitrogen atoms of **7** were refined with isotropic factors.

All the hydrogen atoms of **4** and **6** were located from difference Fourier syntheses and refined isotropically. For **2**, it was not possible to locate with precision hydrogen atoms, but the positive peaks obtained in the final difference Fourier map (up to 1.28 e·Å^{-3}) correspond approximately to the expected positions for the H atoms of the Cp rings. The 13 H atoms of **7** were refined as riding atoms (C–H = 1.08 Å; U_{iso} = 0.075 Å^2).

The results are given in Tables II–IX.

7. Molecular Orbital Analysis. The extended Hückel approach is employed for the study.[21] The atomic parameters for

(19) *International Tables for Crystallography*; Kynoch: Birmingham, 1974; Vol. 4.

(20) Sheldrick, G. M. SHELX 76, Program for Crystal Structure Determinations; University of Cambridge: Cambridge, 1976.

(21) (a) Hoffmann, R.; Lipscomb, W. N. *J. Chem. Phys.* **1962**, *36*, 2179, 3489; **1962**, *37*, 2878. (b) Hoffmann, R. *Ibid.* **1963**, *39*, 1397.

Table II. Fractional Coordinates (×10⁴) and Equivalent Isotropic Temperature Factors (Å²; ×10⁴) with Esd's for 2

atom	x/a	y/b	z/c	U_{eq}
Mo	2342 (1)	2930 (1)	2294 (1)	292 (2)
S(1)	2566 (2)	−955 (2)	3035 (1)	466 (8)
S(2)	2192 (2)	−839 (2)	1336 (1)	792 (14)
C(1)	2345 (5)	238 (8)	2162 (4)	440 (13)
C(2)	2693 (5)	588 (6)	3773 (4)	390 (12)
C(3)	2579 (5)	2182 (8)	3548 (4)	403 (12)
C(4)	2950 (6)	−182 (9)	4627 (4)	495 (15)
C(5)	2633 (8)	3473 (10)	4174 (6)	646 (20)
F(41)	2221 (4)	401 (6)	4860 (3)	866 (33)
F(42)	4096 (4)	105 (6)	5313 (3)	748 (29)
F(43)	2784 (6)	−1780 (5)	4569 (3)	973 (38)
F(51)	3534 (6)	3320 (6)	4994 (3)	1077 (43)
F(52)	2679 (6)	4997 (5)	3949 (4)	1434 (50)
F(53)	1604 (6)	3461 (8)	4174 (5)	1533 (58)
C(11)	4372 (6)	2186 (8)	2853 (4)	484 (13)
C(12)	4465 (6)	3411 (9)	3438 (5)	526 (16)
C(13)	3926 (6)	4893 (9)	2947 (4)	535 (16)
C(14)	3526 (6)	4566 (9)	2045 (5)	530 (16)
C(15)	3784 (6)	2895 (9)	1975 (5)	536 (15)
C(21)	632 (6)	2901 (10)	862 (5)	619 (18)
C(22)	258 (6)	2120 (10)	1386 (5)	643 (19)
C(23)	336 (8)	3272 (10)	1994 (5)	676 (21)
C(24)	752 (6)	4800 (10)	1870 (5)	676 (21)
C(25)	911 (6)	4580 (10)	1165 (5)	605 (18)

Table III. Interatomic Distances (Å), Bond Angles (deg), Mean Planes, and Dihedral Angles (deg) with Esd's in Parentheses for 2

a. Interatomic Distances

Mo–C(1)	2.185 (6)	C(3)–C(5)	1.513 (10)
C(1)–S(1)	1.735 (6)	C(4)–F(41)	1.327 (7)
S(1)–C(2)	1.765 (6)	C(4)–F(42)	1.311 (7)
C(2)–C(3)	1.331 (8)	C(4)–F(43)	1.301 (8)
C(3)–Mo	2.201 (6)	C(5)–F(51)	1.273 (9)
C(1)–S(2)	1.643 (6)	C(5)–F(52)	1.308 (9)
C(2)–C(4)	1.519 (8)	C(5)–F(53)	1.341 (10)
Ring 1 [C(11)–C(15)]		Ring 2 [C(21)–C(25)]	
C(11)–C(12)	1.404 (9)	C(21)–C(22)	1.439 (10)
C(12)–C(13)	1.415 (9)	C(22)–C(23)	1.400 (10)
C(13)–C(14)	1.432 (9)	C(23)–C(24)	1.415 (11)
C(14)–C(15)	1.413 (9)	C(24)–C(25)	1.420 (10)
C(15)–C(11)	1.437 (9)	C(25)–C(21)	1.428 (10)
mean	1.420 (9)	mean	1.420 (10)
Mo–C(11)	2.310 (6)	Mo–C(21)	2.263 (7)
Mo–C(12)	2.362 (7)	Mo–C(22)	2.328 (8)
Mo–C(13)	2.322 (7)	Mo–C(23)	2.363 (8)
Mo–C(14)	2.263 (8)	Mo–C(24)	2.312 (8)
Mo–C(15)	2.260 (7)	Mo–C(25)	2.258 (7)
mean	2.303 (7)	mean	2.305 (8)
Mo–G(1)[a]	1.961	Mo–G(2)[a]	1.963

b. Bond Angles

C(3)–Mo–C(1)	80.4 (2)	S(1)–C(1)–S(2)	114.3 (4)
Mo–C(1)–S(1)	117.5 (3)	S(1)–C(2)–C(4)	110.8 (4)
C(1)–S(1)–C(2)	101.4 (3)	C(4)–C(2)–C(3)	129.0 (5)
S(1)–C(2)–C(3)	120.1 (5)	C(2)–C(3)–C(5)	118.9 (6)
C(2)–C(3)–Mo	120.1 (4)	C(5)–C(3)–Mo	120.5 (5)
Mo–C(1)–S(2)	128.2 (3)	G(1)–Mo–G(2)[a]	141.3

c. Mean Planes

	planarity, Å
P1: ring 1 [C(11)–C(15)]	0.01
P2: ring 2 [C(21)–C(25)]	0.01
P3: Mo,S(1),S(2),C(1),C(2),C(3)	0.03

d. Dihedral Angles

P1–P2	43.9 (5)	P1–P3	19.7 (5)	P2–P3	24.2 (5)

[a] G(1) and G(2) = gravity centers of the cyclopentadienyl rings.

Mo, S, C, and H atoms are tabulated in Table X. Some important geometrical data used in the calculations are listed below.

$Cp_2Mo(\eta^2\text{-}CS_2)$: d(Mo–C(Cp)) = 2.20 Å, d(Mo–C(S)) = 2.1 Å, d(Mo–S_{endo}) = 2.435 Å, ∠Mo–C(S)–S_{exo} = 140°, ∠Mo–C(S)–S_{endo} = 80°.

Table IV. Fractional Coordinates and Equivalent Isotropic Temperature Factors (Å²) with Esd's for 4

atom	x/a	y/b	z/c	B_{eq}
Mo(1)	−0.28908 (3)	−0.27501 (2)	−0.30921 (2)	2.337 (5)
Mo(2)	−0.32693 (3)	0.22471 (2)	−0.32474 (2)	2.265 (5)
S(1)	0.1267 (1)	−0.05025 (6)	0.60592 (7)	4.18 (2)
S(2)	−0.1651 (1)	−0.18588 (6)	−0.41395 (5)	3.08 (2)
S(11)	0.2323 (1)	0.46593 (6)	0.64322 (7)	3.89 (2)
S(12)	0.4715 (1)	0.31944 (6)	0.59205 (5)	3.27 (2)
O(1)	−0.2353 (5)	−0.0965 (2)	0.9038 (2)	7.61 (8)
O(2)	−0.0704 (4)	0.2183 (2)	0.9166 (2)	5.34 (6)
O(3)	0.0599 (5)	0.0404 (2)	−0.1908 (2)	7.46 (8)
O(4)	0.2196 (3)	−0.0762 (2)	−0.1521 (2)	4.19 (5)
O(11)	−0.2310 (4)	0.3558 (2)	−0.0934 (2)	6.12 (7)
O(12)	−0.4500 (4)	0.2580 (2)	−0.0891 (2)	6.44 (7)
O(13)	−0.5496 (4)	0.5188 (2)	−0.1447 (2)	5.77 (6)
O(14)	0.2559 (3)	0.4093 (2)	0.8659 (2)	5.17 (6)
C(1)	−0.5112 (4)	−0.2297 (3)	−0.2300 (2)	4.28 (8)
C(2)	−0.4901 (4)	−0.1630 (2)	−0.2882 (3)	4.58 (8)
C(3)	−0.5368 (4)	−0.2055 (3)	−0.3730 (2)	5.38 (9)
C(4)	−0.5806 (4)	−0.2952 (3)	−0.3685 (3)	4.86 (9)
C(5)	−0.5673 (4)	−0.3093 (3)	−0.2797 (3)	4.39 (8)
C(6)	−0.1961 (6)	−0.3988 (3)	−0.2379 (3)	6.3 (1)
C(7)	−0.0475 (5)	−0.3551 (3)	−0.2508 (3)	5.5 (1)
C(8)	−0.0387 (4)	−0.3541 (3)	−0.3369 (3)	5.17 (9)
C(9)	−0.1858 (6)	−0.4019 (3)	−0.3829 (3)	6.7 (1)
C(10)	−0.2821 (5)	−0.4292 (3)	−0.3167 (4)	7.7 (1)
C(11)	−0.0128 (4)	−0.1139 (2)	0.6494 (2)	2.63 (6)
C(12)	−0.0213 (4)	−0.1114 (2)	0.7438 (2)	2.80 (6)
C(13)	−0.1320 (4)	−0.1690 (2)	−0.2241 (2)	2.83 (6)
C(14)	−0.1512 (5)	−0.1557 (3)	0.8710 (2)	4.01 (8)
C(15)	−0.0901 (7)	−0.2101 (4)	0.0096 (3)	7.5 (1)
C(16)	0.0876 (5)	−0.0392 (2)	−0.1971 (2)	3.74 (7)
C(17)	0.3337 (6)	−0.0128 (3)	−0.0931 (3)	5.53 (9)
C(21)	−0.0463 (5)	0.2519 (3)	−0.2615 (3)	4.88 (9)
C(22)	−0.1055 (4)	0.3368 (3)	−0.2842 (3)	4.43 (8)
C(23)	−0.1397 (5)	0.3329 (3)	−0.3735 (3)	4.53 (8)
C(24)	−0.1064 (5)	0.2472 (3)	−0.4104 (2)	4.90 (8)
C(25)	−0.0424 (4)	0.1962 (3)	−0.3409 (3)	5.4 (1)
C(26)	−0.3851 (6)	0.1031 (3)	−0.2527 (3)	5.24 (9)
C(27)	−0.5477 (5)	0.1379 (2)	−0.2789 (3)	5.09 (9)
C(28)	−0.5733 (5)	0.1270 (3)	−0.3689 (3)	5.71 (9)
C(29)	−0.4284 (6)	0.0875 (3)	−0.3993 (3)	6.4 (1)
C(30)	−0.3160 (5)	0.0709 (2)	−0.3280 (4)	6.1 (1)
C(31)	−0.6181 (4)	0.3901 (2)	−0.3305 (2)	2.67 (6)
C(32)	−0.5504 (4)	0.3797 (2)	−0.2404 (2)	2.72 (6)
C(33)	−0.4289 (4)	0.3172 (2)	−0.2225 (2)	2.86 (6)
C(34)	−0.3563 (5)	0.3151 (3)	−0.1293 (2)	3.99 (7)
C(35)	−0.3981 (9)	0.2529 (4)	0.0032 (3)	9.7 (2)
C(36)	0.3852 (4)	0.4451 (2)	0.8308 (2)	3.21 (6)
C(37)	0.1846 (6)	0.4681 (3)	0.9348 (3)	7.5 (1)

$Cp_2Mo(CS_2C_2H_2)$, metallacycle C: d(Mo–C_2) = 2.164°, d(C–C_1) = 1.5 Å, ∠C_2–Mo–S_{endo} = 76.7°, ∠Mo–S_{endo}–C = 106.4°, ∠S_{endo}–C–C_1 = 114°, ∠C_2–C_1–C = 120°.

The geometrical parameters used to construct the Walsh diagram in Figure 11 are as follows: α, the angle between the horizontal line and the Mo–S_1 bond; β, the Mo–S_1–C angle; γ, the S_1–C–S_2 angle; δ, the C_1–C–S_1 angle; and d, the C_1–C distance.

Results and Discussion

1. Syntheses. The reaction of $[Mo(\eta^5\text{-}C_5H_5)_2(\eta^2\text{-}CS_2)]$ (1) with hexafluorobut-2-yne ($CF_3C{\equiv}CCF_3$) occurred smoothly at room temperature in THF solution to give, in ca. 30% yield, the green 1:1 adduct **2** for which the inequivalency of the two CF_3 groups, deduced from the ^{19}F NMR data, precluded the metalladithiocarbene A structure (Figure 1). On the basis of ^{13}C NMR data, and particularly from the presence on the spectrum of a very low-field signal at δ 310.3 ppm assigned to a Mo–C(S)–S moiety, type B structure was proposed for **2**.

At room temperature, **1** does not react with dimethyl acetylenedicarboxylate ($CH_3CO_2C{\equiv}CCO_2CH_3$). However, reaction occurred in refluxing THF and after chromatographic separation two distinct compounds were separated: a brown complex (**3**) and a dark green complex (**4**). In both

Table V. Interatomic Distances (Å), Bond Angles (deg), and Dihedral Angles (deg) with Esd's in Parentheses for 4[a]

	I	II
	a. Interatomic Distances	
Mo(1)-S(2)	2.440 (1)	2.442 (1)
S(2)-C(11)	1.713 (2)	1.705 (2)
C(11)-C(12)	1.460 (3)	1.454 (3)
C(12)-C(13)	1.354 (3)	1.344 (3)
C(13)-Mo	2.183 (2)	2.187 (2)
C(11)-S(1)	1.649 (2)	1.656 (2)
C(12)-C(16)	1.502 (3)	1.508 (3)
C(16)-O(3)	1.185 (3)	1.192 (3)
C(16)-O(4)	1.319 (3)	1.308 (3)
O(4)-C(17)	1.444 (3)	1.456 (4)
C(13)-C(14)	1.482 (3)	1.487 (3)
C(14)-O(1)	1.191 (4)	1.177 (4)
C(14)-O(2)	1.332 (3)	1.337 (4)
O(2)-C(15)	1.450 (4)	1.446 (5)
ring 1 [C(1)-C(5)]		
C-C mean	1.387 (5) [from 1.364 (5) to 1.413 (4)]	1.368 (6) [from 1.339 (5) to 1.410 (7)]
Mo-C mean	2.301 (3) [from 2.267 (3) to 2.339 (3)]	2.299 (3) [from 2.253 (3) to 2.353 (3)]
Mo-G(1)[b]	1.975 (3)	1.978 (3)
Ring 2 [C(6)-C(10)]		
C-C mean	1.389 (5) [from 1.363 (5) to 1.418 (5)]	1.372 (5) [from 1.365 (6) to 1.388 (5)]
Mo-C mean	2.304 (3) [from 2.260 (3) to 2.357 (3)]	2.294 (3) [from 2.253 (3) to 2.350 (3)]
Mo-G(2)[b]	1.983 (3)	1.976 (3)
	b. Bond Angles	
C(13)-Mo-S(2)	77.3 (2)	76.8 (2)
Mo-S(2)-C(11)	104.2 (3)	104.9 (3)
S(2)-C(11)-C(12)	114.7 (2)	114.8 (2)
C(11)-C(12)-C(13)	120.6 (2)	120.7 (2)
C(12)-C(13)-Mo	121.9 (2)	122.7 (3)
S(2)-C(11)-S(1)	122.0 (2)	122.2 (2)
S(1)-C(11)-C(12)	123.3 (2)	123.0 (2)
C(11)-C(12)-C(16)	117.8 (2)	117.3 (2)
C(12)-C(16)-O(3)	125.2 (2)	124.0 (2)
O(3)-C(16)-O(4)	123.9 (4)	123.9 (2)
C(16)-O(4)-C(17)	115.6 (2)	115.8 (2)
C(16)-C(12)-C(13)	121.5 (2)	121.9 (2)
C(12)-C(13)-C(14)	118.2 (2)	117.7 (2)
C(13)-C(14)-O(1)	123.5 (3)	126.3 (3)
O(1)-C(14)-O(2)	122.6 (3)	122.3 (3)
C(14)-O(2)-C(15)	116.0 (3)	116.9 (3)
G(1)-Mo-G(2)	137.8 (4)	139.0 (4)
	c. Dihedral Angles	
P1, Mo,S(2),C(11),C(12),C(13); P(2), ring 1; P(3), ring 2		
P1-P2	26.6	24.5
P1-P3	18.1	22.2
P2-P3	44.7	46.7

[a] (I) and (II): values for the two independent molecules. [b] G(1) and G(2): gravity centers of the cyclopentadienyl rings.

cases, analytical and mass spectral data were in agreement with formation of 1:1 adducts. These two isomers were easily differentiated from IR and ^1H NMR data. However, the main spectroscopic difference concerned the ^{13}C NMR data: only **3** exhibited a low-field signal (δ 313.1 ppm) comparable to that observed in **2** while for **4** the lower field peak was pointed out at δ 246.7 ppm. Therefore, these data suggested a type B structure for **3** and a type C structure for **4**.

It is noteworthy that formation of two isomeric heterometallacycles $[Cp_2\overline{TiSC(R)=C(R)S}]$ and $[Cp_2\overline{TiSSC(R)=CR}]$ (R = CO_2Me) has been reported previously from reactions of $[Cp_2TiS_x]_n$ with DMAD.[22]

Table VI. Fractional Coordinates and Equivalent Isotropic Temperature Factors (Å^2) with Esd's for 6

atom	x/a	y/b	z/c	B_{eq}
Mo	0.05856 (4)	0.19777 (3)	0.13582 (2)	2.487 (7)
Cl(1)	0.2048 (3)	0.4556 (2)	0.0185 (2)	10.87 (8)
Cl(2)	0.4786 (3)	0.3832 (2)	0.0694 (2)	13.4 (1)
S(1)	−0.1053 (1)	0.10076 (9)	0.29994 (8)	3.50 (2)
S(2)	0.1266 (1)	0.00562 (8)	0.26573 (8)	3.24 (2)
O(1)	0.2760 (3)	−0.1276 (2)	0.2156 (3)	4.37 (8)
O(2)	0.3751 (3)	−0.0569 (2)	0.1194 (2)	4.27 (8)
O(3)	0.3746 (3)	0.1392 (2)	0.0761 (2)	4.46 (8)
O(4)	0.2242 (4)	0.0639 (3)	−0.0283 (2)	4.97 (9)
N	−0.4641 (5)	0.0910 (4)	0.3215 (4)	7.3 (2)
C(1)	−0.1521 (5)	0.2399 (5)	0.0575 (4)	5.7 (2)
C(2)	−0.0559 (7)	0.2872 (4)	0.0256 (4)	5.8 (2)
C(3)	0.0146 (6)	0.2289 (5)	−0.0157 (3)	5.1 (1)
C(4)	−0.0402 (5)	0.1471 (4)	−0.0096 (4)	4.8 (1)
C(5)	−0.1409 (5)	0.1538 (4)	0.0346 (4)	4.9 (1)
C(6)	0.2424 (4)	0.2040 (3)	0.2569 (3)	3.06 (9)
C(7)	0.2376 (5)	0.2846 (3)	0.2126 (3)	3.5 (1)
C(8)	0.1137 (5)	0.3255 (3)	0.2144 (3)	3.6 (1)
C(9)	0.0397 (4)	0.2695 (3)	0.2580 (3)	3.3 (1)
C(10)	0.1166 (4)	0.1899 (3)	0.2816 (3)	3.01 (9)
C(11)	0.0436 (4)	0.1086 (3)	0.2576 (3)	2.84 (9)
C(12)	−0.2090 (5)	0.0376 (3)	0.2175 (3)	3.7 (1)
C(13)	−0.3366 (5)	0.0223 (4)	0.2113 (4)	4.2 (1)
C(14)	−0.4062 (5)	0.0596 (4)	0.2726 (4)	5.0 (1)
C(15)	0.2046 (4)	0.0164 (3)	0.1745 (3)	2.74 (9)
C(16)	0.1863 (4)	0.0862 (3)	0.1204 (3)	2.66 (9)
C(17)	0.2623 (5)	0.0926 (3)	0.0478 (3)	3.6 (1)
C(18)	0.4565 (6)	0.1446 (5)	0.0105 (4)	6.5 (2)
C(19)	0.2956 (4)	−0.0579 (3)	0.1653 (3)	3.2 (1)
C(20)	0.3540 (6)	−0.2047 (4)	0.2076 (4)	5.5 (1)
C(30)	0.3525 (9)	0.406 (1)	−0.0033 (5)	20.9 (6)

Unambiguous confirmations of the presence of these two different metallacycles, $\overline{MoC(S)SC(R)=CR}$ in **2** and $\overline{MoSC(S)C(R)=CR}$ in **4**, were obtained from X-ray crystal structure determinations (see below).

In order to search for new types of combination of CS_2 with two (or more) alkynes, these 1:1 adducts were further reacted with alkynes.

We look at, with special interest, their reactions with cyanoethyne HC≡CCN since, among the alkynes activated by electron-withdrawing groups, previous studies[23] have shown that the cyanoalkynes (HC≡CCN and NCC≡CCN) often present high and peculiar reactivities presumably due to (i) a high electron affinity of the nitrile group, (ii) an important and highly delocalized π-electron system, and (iii) low steric constraints arising from the small CN group.

While reaction of HC≡CCN with the type C complex **4** gave a complex manifold of products, the separation of which as pure samples could not be achieved, such a reaction with type B complexes (**2** and **3**) interestingly afforded novel compounds (Figure 2).

Reaction of **2** with a large excess of HC≡CCN (CH_2Cl_2, 24 h at room temperature) gave, after further workup, the new compound **5** as red-orange microcrystals in 55% yield. Analytical data for **5** were indicative of the formation of a 1:1 adduct between **2** and the cyanoalkyne. Although the ^1H NMR spectrum exhibited remarkable, features (i) a doublet of doublets assignable to a (*Z*)-CNCH=CH- alkenyl unit and (ii) cyclopentadienyl signals indicating the loss of one proton for one of the two C_5H_5 groups, the molecular structure of **5** could not be elucidated in absence of suitable crystals for an X-ray study.

(22) Giolando, D. M.; Rauchfuss, T. B.; Rheingold, A. L.; Wilson, S. R. *Organometallics* **1987**, *6*, 667 and references therein.

(23) See, for instance: Scordia, H.; Kergoat, R.; Kubicki, M. M.; Guerchais, J. E. *J. Organometal. Chem.* **1983**, *249*, 371.

Table VII. Interatomic Distances (Å), Bond Angles (deg), and Mean Planes with Esd's in Parentheses for 6

a. Interatomic Distances

Mo–C(11)	2.324 (4)	C(11)–S(2)	1.776 (4)
S(2)–C(15)	1.762 (3)	C(15)–C(16)	1.328 (5)
C(16)–Mo	2.192 (3)	C(11)–S(1)	1.796 (3)
C(11)–C(10)	1.448 (5)	S(1)–C(12)	1.725 (4)
C(12)–C(13)	1.308 (5)	C(13)–C(14)	1.419 (7)
C(14)–N	1.158 (6)	C(16)–C(17)	1.495 (5)
C(17)–O(3)	1.333 (5)	C(17)–O(4)	1.207 (4)
O(3)–C(18)	1.448 (5)	C(15)–C(19)	1.494 (5)
C(19)–O(1)	1.350 (5)	C(19)–O(2)	1.191 (4)
O(1)–C(20)	1.443 (5)	C(30)–Cl(1)	1.794 (11)
C(30)–Cl(2)	1.522 (9)		
	C(1)–C(5) Ring		
C(1)–C(2)	1.397 (8)	Mo–C(1)	2.291 (4)
C(2)–C(3)	1.386 (7)	Mo–C(2)	2.254 (4)
C(3)–C(4)	1.379 (7)	Mo–C(3)	2.279 (4)
C(4)–C(5)	1.363 (7)	Mo–C(4)	2.323 (4)
C(5)–C(1)	1.369 (8)	Mo–C(5)	2.339 (4)
mean	1.379 (9)	mean	2.297 (4)
	C(6)–C(10) Ring		
C(6)–C(7)	1.395 (5)	Mo–C(6)	2.294 (3)
C(7)–C(8)	1.420 (6)	Mo–C(7)	2.333 (4)
C(8)–C(9)	1.407 (6)	Mo–C(8)	2.281 (4)
C(9)–C(10)	1.444 (5)	Mo–C(9)	2.197 (4)
C(10)–C(6)	1.442 (5)	Mo–C(10)	2.148 (3)

b. Bond Angles

C(16)–Mo–C(11)	77.6 (2)	Mo–C(11)–S(2)	116.8 (2)
C(11)–S(2)–C(15)	99.4 (2)	S(2)–C(15)–C(16)	122.3 (3)
C(15)–C(16)–Mo	123.8 (2)	S(2)–C(15)–C(19)	114.4 (3)
C(19)–C(15)–C(16)	123.3 (3)	C(15)–C(16)–C(17)	118.9 (3)
S(1)–C(11)–S(2)	110.5 (2)	S(1)–C(11)–C(10)	113.5 (2)
S(2)–C(11)–C(10)	122.0 (2)	C(11)–S(1)–C(12)	102.0 (2)
S(1)–C(12)–C(13)	125.6 (3)	C(12)–C(13)–C(14)	122.2 (4)
C(13)–C(14)–N	178.8 (5)	C(16)–C(17)–O(3)	111.2 (3)
C(16)–C(17)–O(4)	125.0 (4)	O(3)–C(17)–O(4)	123.7 (3)
C(17)–O(3)–C(18)	114.1 (4)	C(15)–C(19)–O(2)	125.1 (4)
C(15)–C(19)–O(1)	111.3 (3)	O(1)–C(19)–O(2)	123.6 (3)
C(19)–O(1)–C(20)	115.7 (3)	Cl(1)–C(30)–Cl(2)	124.7 (4)
	C(1)–C(5) and C(6)–C(10) Rings		
C(5)–C(1)–C(2)	107.4 (5)	C(10)–C(6)–C(7)	108.9 (3)
C(1)–C(2)–C(3)	108.2 (5)	C(6)–C(7)–C(8)	107.9 (4)
C(2)–C(3)–C(4)	106.6 (4)	C(7)–C(8)–C(9)	109.1 (4)
C(3)–C(4)–C(5)	109.5 (5)	C(8)–C(9)–C(10)	107.6 (3)
C(4)–C(5)–C(1)	108.4 (5)	C(9)–C(10)–C(6)	106.2 (3)
mean	108.0 (5)		

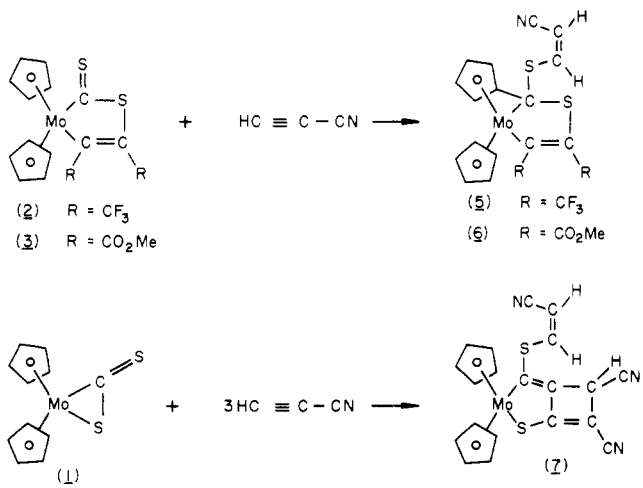

Figure 2. 2:1 and 3:1 adducts between alkyne and an η^2-CS_2 ligand described in this work.

However, reaction of HC≡CCN with **3** afforded **6** for which analytical and spectral data clearly indicated a similar molecular structure to that of **5**. The crystal structure determination of **6** (see below) shows that formations of **5** and **6** from **2** and **3** involve the following unusual features: (i) transformation of one of the two η^5-C_5H_5 ligands into a substituted η^5-C_5H_4 group by cleavage of a C–H bond and formation of a C–C bond between the resulting C_5H_4 moiety and the carbon atom of the η^2-CS_2 unit (ultimately the coupling product between the cyclopentadienyl ring and the substituted CS_2 fragment results in a type of fulvene ligand, already shown apt to coordinate the Mo and W metals[24]); (ii) addition on the uncoordinated sulfur atom of the alkenyl fragment arising from addition of an H atom onto the alkyne.

Table VIII. Fractional Coordinates (×10⁴) and Equivalent Isotropic Temperature Factors (Å²; ×10⁴) for 7

atom	*x/a*	*y/b*	*z/c*	U_{eq}
Mo	1287 (1)	536 (1)	1837 (1)	346 (6)
S(1)	2423 (2)	638 (4)	1648 (2)	477 (26)
S(2)	977 (2)	−505 (5)	3829 (2)	556 (28)
C(1)	1567 (6)	−67 (11)	3129 (8)	330 (36)
C(11)	1254 (6)	−355 (13)	4857 (8)	485 (41)
C(12)	939 (6)	−780 (13)	5530 (10)	517 (49)
C(13)	384 (8)	−1418 (15)	5448 (10)	522 (49)
N(1)	−42 (6)	−1969 (12)	5382 (8)	690 (15)
C(21)	2150 (6)	−31 (12)	3297 (9)	362 (39)
C(22)	2641 (6)	−171 (12)	3983 (8)	339 (41)
C(23)	2726 (6)	−1460 (15)	4325 (9)	473 (47)
N(2)	2780 (6)	−2436 (13)	4593 (8)	624 (14)
C(31)	2603 (6)	299 (13)	2673 (8)	358 (40)
C(32)	3071 (6)	186 (12)	3248 (9)	399 (40)
C(33)	3693 (8)	375 (15)	3196 (10)	647 (44)
N(3)	4210 (6)	513 (16)	3152 (10)	630 (16)
C(41)	1527 (6)	2611 (15)	2073 (10)	670 (55)
C(42)	1099 (6)	2276 (15)	2707 (11)	615 (57)
C(43)	607 (9)	1916 (16)	2381 (12)	740 (58)
C(44)	609 (9)	2105 (16)	1516 (11)	766 (65)
C(45)	1191 (8)	2528 (16)	1298 (11)	724 (59)
C(51)	599 (8)	−1050 (13)	1791 (11)	627 (52)
C(52)	579 (8)	−403 (16)	1021 (10)	670 (51)
C(53)	1124 (6)	−558 (17)	591 (9)	568 (45)
C(54)	1516 (8)	−1304 (13)	1068 (10)	607 (53)
C(55)	1178 (8)	−1633 (15)	1802 (12)	643 (51)

These surprising results prompted us to examine the reaction of HC≡CCN with [Mo(η^5-C_5H_5)$_2$(η^2-CS_2)] (**1**). We anticipated that such a reaction might give either 1:1 adducts of types B and C (as **3** and **4**, respectively) or a 2:1 adduct similar to **5** and **6** (Figure 2). However, a quite different product is formed instead.

1 reacted with a large excess of HC≡CCN (THF, room temperature for ca. 40 h) affording complex **7**, the analytical data of which unambiguously indicated formation of a 3:1 adduct. The structure of **7** has been established by X-ray study. It is noteworthy that the uncoordinated metal sulfur atom of **7** bears a (*Z*)-CNCH=CH-alkenyl group as in **5** and **6** (Figure 2). However, in contrast with the formations of **5** and **6**, that of **7** involves two striking differences: (i) the [Mo(η^5-C_5H_5)$_2$] fragment remains intact and (ii) there is cleavage of the C–S bond of the [Mo(η^2-CS_2)] moiety to generate a –S–Mo–C–S unit. As shown below, the rather uncommon organic skeleton of **7** may be viewed as a substituted cyclobutene [C(21)C(22)C(32)=C(31); see labeling scheme, Figure 3] or as a substituted butadiene [C(1)=C(21)C(31)=C(32)].

It is not yet clear how this unexpected complex **7** was formed in the reaction of **1** with HC≡CCN since all attempts to isolate an intermediate failed.

It is noteworthy that from a similar reaction performed under different experimental conditions (1:1 ratio, CH_2Cl_2, −20 °C for ca. 4 h), no traces of **7** could be detected. However, this reaction unexpectedly afforded two new

(24) Bandy, J. A.; Mtetwa, V. S. B.; Prout, K.; Green, J. C.; Davies, C. E.; Green, M. L. H.; Hazel, N. J.; Izquierdo, A.; Martin-Polo, J. J. *J. Chem. Soc., Dalton Trans.* **1985**, 2037.

Table IX. Interatomic Distances (Å), Bond Angles (deg), Mean Planes, and Dihedral Angles (deg) with Esd's in Parentheses for 7

a. Interatomic Distances

Mo-S(1)	2.527 (4)	Mo-C(1)	2.211 (13)
S(1)-C(31)	1.693 (12)	C(1)-S(2)	1.767 (13)
C(31)-C(21)	1.443 (16)	C(1)-C(21)	1.314 (15)
C(31)-C(32)	1.377 (17)	C(21)-C(22)	1.535 (17)
C(22)-C(32)	1.539 (17)	C(32)-C(33)	1.391 (18)
C(22)-C(23)	1.490 (18)	C(23)-N(2)	1.132 (17)
C(33)-N(3)	1.156 (18)		
S(2)-C(11)	1.731 (13)	C(11)-C(12)	1.343 (17)
C(12)-C(13)	1.407 (19)	C(13)-N(1)	1.116 (18)
Ring 1		Ring 2	
C(41)-C(42)	1.419 (19)	C(51)-C(52)	1.390 (19)
C(42)-C(43)	1.261 (20)	C(52)-C(53)	1.391 (19)
C(43)-C(44)	1.370 (20)	C(53)-C(54)	1.395 (19)
C(44)-C(45)	1.405 (21)	C(54)-C(55)	1.415 (20)
C(45)-C(41)	1.426 (19)	C(55)-C(51)	1.423 (19)
mean	1.376 (20)	mean	1.403 (20)
Mo-C(41)	2.312 (16)	Mo-C(51)	2.279 (15)
Mo-C(42)	2.346 (16)	Mo-C(52)	2.255 (16)
Mo-C(43)	2.273 (18)	Mo-C(53)	2.304 (15)
Mo-C(44)	2.306 (18)	Mo-C(54)	2.362 (16)
Mo-C(45)	2.303 (17)	Mo-C(55)	2.334 (15)
mean	2.308 (17)	mean	2.307 (16)

b. Bond Angles

S(1)-Mo-C(1)	81.0 (0.4)	Mo-S(1)-C(31)	96.4 (0.5)
Mo-C(1)-C(21)	116.7 (1.0)	Mo-C(1)-S(2)	116.1 (0.7)
S(2)-C(1)-C(21)	127.3 (1.2)	S(1)-C(31)-C(21)	122.2 (1.1)
C(1)-C(21)-C(31)	123.3 (1.4)	S(1)-C(31)-C(32)	144.6 (1.2)
C(1)-C(21)-C(22)	146.2 (1.4)	C(21)-C(31)-C(32)	93.2 (1.1)
C(31)-C(21)-C(22)	90.4 (1.0)	C(31)-C(32)-C(22)	92.8 (1.1)
C(21)-C(22)-C(32)	83.6 (1.0)	C(31)-C(32)-C(33)	133.7 (1.5)
C(21)-C(22)-C(23)	115.4 (1.2)	C(22)-C(32)-C(33)	133.5 (1.4)
C(32)-C(22)-C(23)	114.9 (1.2)		
C(22)-C(23)-N(2)	178.7 (1.8)	C(32)-C(33)-N(3)	179.0 (1.9)
C(1)-S(2)-C(11)	107.0 (0.7)	S(2)-C(11)-C(12)	121.0 (1.3)
C(11)-C(12)-C(13)	122.9 (1.5)	C(12)-C(13)-N(1)	177.2 (1.9)

c. Equations of Least-Squares Planes[a]

plane	atoms in plane	*A*	*B*	*C*	*D*	planarity, Å
P(1)	Mo, S(1), S(2), C(1)	-0.0107	0.9454	0.3258	-1.4476	0.04
P(2)	S(1), S(2), C(1), C(21) C(22), C(31), C(32), C(33), N(3)	-0.1063	0.9639	0.2443	-0.7276	0.03
P(3)	C(41), C(42), C(43), C(44), C(45)	-0.3148	0.9426	0.1112	-1.9544	0.04
P(4)	C(51), C(52), C(53), C(54), C(55)	0.3675	0.8072	0.4619	-0.8643	0.02

d. Distances (×10³; Å) from the Least-Squares Planes

from P(1) Mo 2; S(1) 19; S(2) -28; C(1) 44; C(21) 153; C(31) 158
from P(2) S(1) -8; S(2) -13; C(1) 32; C(21) 3; C(22) 1; C(31) 8; C(32) 14; C(33) 15; N(3) 19, Mo 225
from P(3) C(41) -22; C(42) 49; C(43) -29; C(44) 9; C(45) 7
from P(4) C(51) 11; C(52) -3; C(53) 6; C(54) 13; C(55) -14

e. Interplanar Angles

P(1)-P(2)	7.2	P(1)-P(3)	21.5
P(1)-P(4)	24.5	P(3)-P(4)	45.8

[a] The equations are of the form $Ax + By + Cz + D = 0$ where x, y, z (in Å) refer to the orthogonal system a, b, c.

compounds, **8** and **9**. **8**, which was obtained in ca. 20% yield, gave a ^1H NMR spectrum with only a single resonance (in the Cp range). Analytical and spectroscopic data showed that **8** is the trithiocarbonato derivative [Mo(η^5-C_5H_5)$_2$(η^2-CS_3)]. The IR data [ν(C=S) 1010 (vs br); ν(CS) 865 (m)] were in agreement with previously reported values for η^2-CS_3 ligand.[25]

Table X. Atomic Parameters Used in the Calculations

atom	orbital	H_{ii}, eV	ζ_1	ζ_2	C_1[a]	C_2[a]
Mo	5s	-8.34	1.96			
	5p	-5.24	1.92			
	4d	-10.50	4.54	1.90	0.5899	0.5899
S	3s	-20.00	1.82			
	3p	-13.3	1.82			
C	2s	-21.4	1.62			
	2p	-11.4	1.62			
H	1s	-13.6	1.30			

[a] Coefficients used in double-ζ expansion for d orbitals.

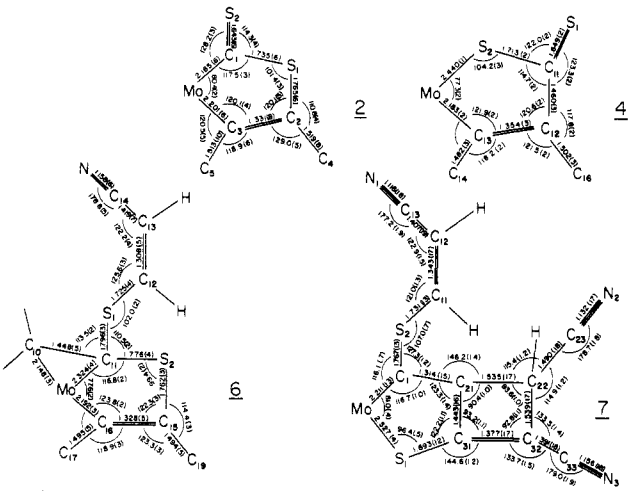

Figure 3. Comparison of the metallacyclic fragments of **2**, **4**, **6**, and **7**.

Elemental analyses indicated that **9**, which is only obtained in very low yield (ca. 3%), is a sulfur-containing organic product of formula $C_6H_4N_2S$. On the basis of ^1H NMR data, its structure was assumed to be [S((*Z*)-CH=CHCN)$_2$].

Obviously, the unexpected formations of **8** and **9** in the reaction between **1** and HC≡CCN gave no information about the mechanism of formation of **7**. However, they show that the reaction of an alkyne with a η^2-CS_2 ligand may be much more complex than previously thought. They particularly confirm that such a reaction may involve some redistribution of the sulfur atoms.[12,25] It is noteworthy that the "carbonato" analogue of **8**, namely, [Mo(η^5-C_5H_5)$_2$(η^2-CO_3)], has been recently obtained by disproportionation of carbon dioxide [irradiation of [$Cp_2Mo(\eta$-$CO_2)$] under 1 atm of CO_2].[26]

2. X-ray Structural Studies. Molecular structures of the 1:1 adducts **2** (type B) and **4** (type C) and the 2:1 (**6**) and 3:1 (**7**) complexes with appropriate numbering schemes are given in Figures 4–7 while atomic coordinates and pertinent bond distances and angles were given in Tables II–IX.

The molecules in all four complexes are separated by van der Waals distances, and no unusually close intermolecular contacts are observed. For **2**, **6**, and **7**, the asymmetric unit contains one molecule at a general position; for **4**, it contains two independent molecules that present very similar features. While the [Mo(η^5-C_5H_5)$_2$] fragments of complexes **2**, **4**, and **7** are unexceptional for $MoCp_2$ derivatives[27] and do not necessitate any further

(25) (a) Benson, I. B.; Hunt, J.; Knox, S. A. R.; Oliphant, V. *J. Chem. Soc., Dalton Trans.* **1978**, 1240. (b) Doherty, J.; Fortune, J.; Manning, A. R.; Stephens, F. S. *J. Chem. Soc., Dalton Trans.* **1984**, 1111. (c) Bianchini, C.; Meli, A.; Vizza, F. *Angew. Chem. Int. Ed. Engl.* **1987**, *26*, 767.

(26) Belmore, K. A.; Vanderpool, R. A.; Tsai, J. C.; Khan, M. A.; Nicholas, K. M. *J. Am. Chem.* **1988**, *110*, 2004.

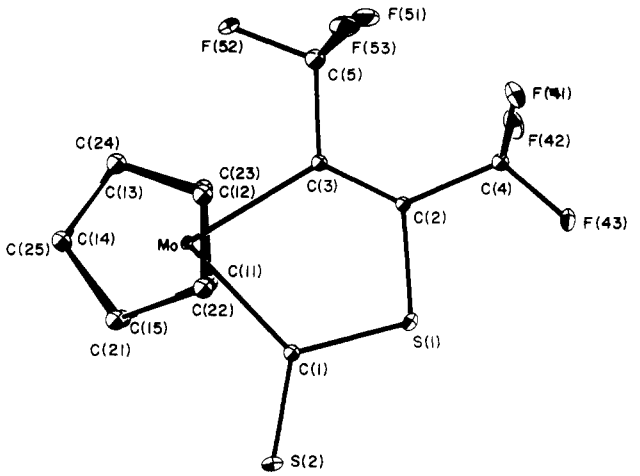

Figure 4. Molecular structure of **2**: ORTEP projections on the mean plane of the organic framework. The ellipsoids and spheres (C atoms) include a probability of 25%.

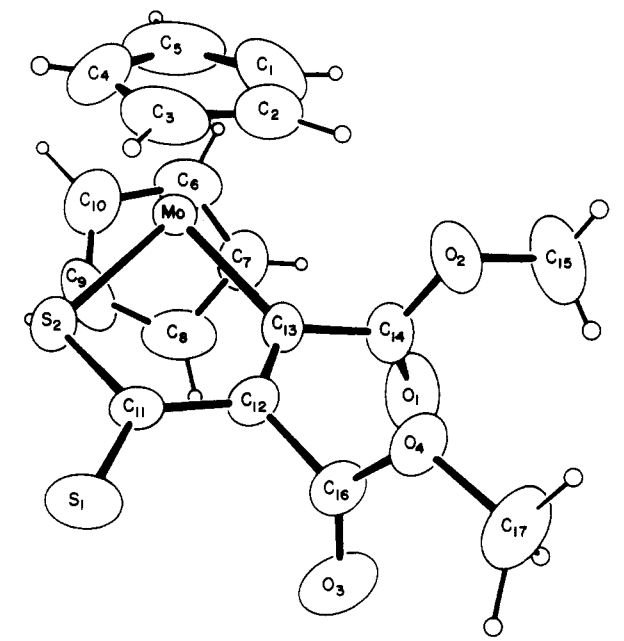

Figure 5. Molecular structure of one of two crystallographically distinct molecules of **4** (the other independent molecule shows similar features). Non-hydrogen atoms are shown as 50% thermal ellipsoids. The hydrogen atoms have been arbitrarily assigned artificially small thermal parameters.

comment, the geometric changes arising from the coupling reaction between one of the C_5H_5 ligands and the carbon atom of the metallacycle observed in the formation of **6** will be carefully studied (see below).

1:1 (η^2-CS_2)-Alkyne Adducts 2 and 4. The X-ray studies, which unequivocally confirm that **2** and **4** are respectively type B and type C complexes (see Figure 1), also show that the two fragments of particular interest ($\overline{MoCSC{=}C}$ in **2**; $\overline{MoSCC{=}C}$ in **4**) both present the following features (see also Figure 3).

(i) These fragments are found to be planar within 0.03 Å, and their plane approximately bisects the $MoCp_2$ moiety.

(ii) The carbon–carbon bonds arising from the alkynes are very similar [1.331 (8) Å in **2**; 1.354 (3) Å in **4**]; both are of double-bond character.

(27) Prout, K.; Cameron, T. S.; Forder, A.; Critchley, S. R.; Denton, B.; Rees, G. V. *Acta Crystallogr., Sect. B* **1974**, *B30*, 2290.

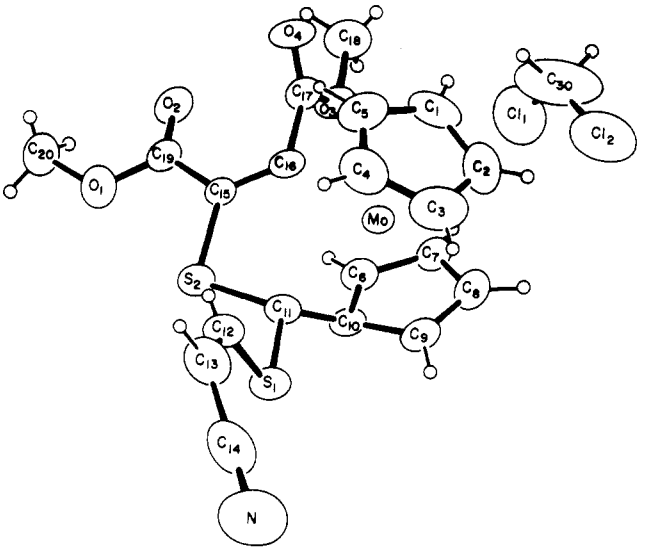

Figure 6. Molecular structure of **6**. Non-hydrogen atoms are shown as 50% thermal ellipsoids. The hydrogen atoms have been arbitrarily assigned artificially small thermal parameters.

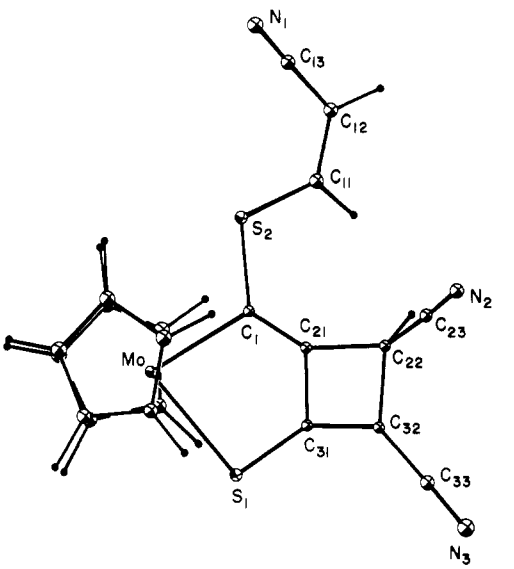

Figure 7. Molecular structure of **7**: ORTEP projection on the mean plane of the organic framework. Non-hydrogen atoms are shown as 30% thermal ellipsoids or spheres. The hydrogen atoms have been arbitrarily assigned artificially small thermal parameters.

(iii) The endocyclic carbon–sulfur bonds arising from the η^2-CS_2 ligand [1.735 (6) Å in **2**; 1.713 (2) Å in **4**] exhibit some multiple-bond character since the usual length for a pure σ C—S bond is considered to be about 1.81 Å while the C=S double bond length in free CS_2 is 1.554 Å.[28] This multiple-bond character is obviously much more important for the exocyclic carbon–sulfur bonds which also display similar lengths [1.643 (6) Å in **2**; 1.649 (2) Å in **4**].

(iv) The three molybdenum–carbon distances [Mo–C(S) = 2.185 (6) Å and Mo–C(C) = 2.201 (6) Å in **2**; Mo–C(C) = 2.183 (2) Å in **4**] are shorter than the Mo–CH_2 distance found in $[Mo(\eta^5\text{-}C_5H_5)_2(C_2H_5)Cl]$[27] and virtually identical with those in $[MoO_2(CH_3)_2(bpy)]$ (2.20 Å).[29] They are indicative of partial double-bond character and appear to be the result of a delocalization of the π-electron system over all of the metallacyclic fragments, as also shown by

(28) (a) Hyde, J.; Venkatasubramanian, K.; Zubieta, J. *Inorg. Chem.* **1978**, *17*, 414. (b) Guenther, A. H. *J. Chem. Phys.* **1959**, *31*, 1095.

(29) Schrauzer, G. N.; Hughes, L. A.; Strampach, N.; Robinson, P. R.; Schlemper, E. O. *Organometallics* **1982**, *1*, 44.

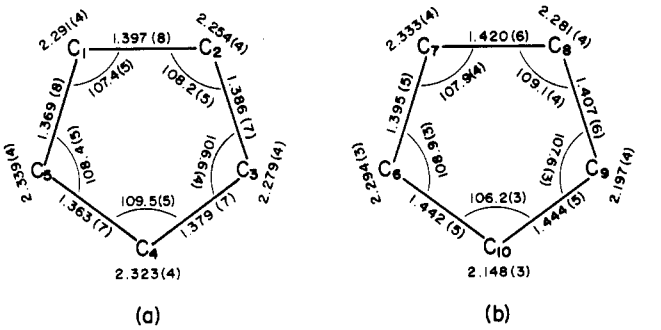

Figure 8. Carbon–carbon, carbon–molybdenum bond lengths (Å), and internal cyclic CCC angles (deg) for the "normal" η^5-C_5H_5 (a) and the "substituted" C_5H_4 ligands in **6**.

the C(2)–S(1) bond length in **2** and the C(11)–C(12) distance in **4**.

2:1 (η^2-CS_2)–Alkyne Adduct 6. The striking features of **6** arise from the unexpected carbon–carbon bond between the carbon atom C(10) of the cyclopentadienyl group and the carbon atom C(11) bonded to the molybdenum. The formation "in situ" of a fulvene ligand is readily envisaged by the structural similarities with the complex $[(\eta^6\text{-}C_6H_6)\overline{Mo(\eta^6\text{-}C_5H_4CPh_2)}]$ (**10**) recently prepared by reaction of $[Mo(\eta^6\text{-}C_6H_6)_2]$ with 6,6-diphenylfulvene.[24] As in **10**, the exocyclic C(10)–C(11) bond is not coplanar with the C_5 ring but forms with it a "dip" angle of ca. 40°. Also the latter exocyclic bond displays some sign of multiple bonding [1.448 (5) Å in **6**, 1.437 (4) Å in **10**]. Finally, the coordination of C(10)–C(11) to the metal disturbs the geometry of the MoCp fragment (Figure 8) since the Mo–C(10) bond [2.148 (3) Å] appears stronger than the four other Mo–C bonds of the "substituted" Cp rings [from 2.197 (4) to 2.333 (4) Å; mean value 2.276 (4) Å], the latter being only very slightly affected since the five Mo–C bonds of the "normal" η^5-Cp ligand in **6** [from 2.254 (4) to 2.339 (4) Å] present an average value of 2.297 (4) Å. Perturbations also appear in the C_5 carbon skeleton itself [Figure 8], the two C–C bonds from C(10) [1.442 (5) and 1.444 (5) Å] being significantly longer than the mean value [1.407 (6) Å] of the other three C–C bonds in the "substituted" C(6)···C(10) cyclopentadienyl ring [for the "normal" C(1)···(5) cyclopentadienyl ligand, C–C mean value = 1.379 (9) Å]. A theoretical analysis of the bonding capabilities of the fulvene ligand is also presented in ref 30.

The $\overline{MoCSC{=}C}$ metallaheterocycle itself is not very much affected by the creation of this extra C–C bond and presents features similar to those of the corresponding fragment in **2**, if we exclude the lengthening of the M–C(S) bond. The value found for **6** [Mo–C(11) = 2.324 (4) Å] is significantly greater than the corresponding bond in **2** [Mo–C(1) = 2.185 (6) Å] and seems to be indicative of a pure σ M–C bond arising from the breakdown of the π delocalization by the (sp^3)C(11)–S(2) bond. Interestingly, the sp^2 hybridization of the carbon atom of the alkyne bound to the endocyclic sulfur atom appears less distorted in **6** than in **2**.

The exocyclic C(11)–S(1) bond [1.796 (3) Å] appears as an almost pure σ C–S bond while the S(1)–C(12) bond [1.725 (4) Å] shows slight multiple character. Bond lengths and angles found in the sulfur-bound alkenyl group are as expected.

3:1 (η^2-CS_2)–Alkyne Adduct 7. As can be seen from Figures 2 and 7, **7** is unique in that it exhibits a rather complex organic fragment, the framework of which presents a nine-atom system S(2)–C(1)–C(21)–C(22)–C(32)[C(33)–N(3)]–C(31)–S(1) planar within 0.03 Å. This skeleton may be considered as two fused rings. The first one, the metallacycle $\overline{MoC(1)C(21)C(31)S(1)}$, includes a strong carbon–carbon double bond C(1)–C(21) [1.314 (15) Å]. The second ring, $\overline{C(21)C(22)C(32)C(31)}$, is a pure organic four-membered cycle. It may be described as a substituted cyclobutene including the C(31)–C(32) double bond [1.377 (17) Å] and rather unusual and very distorted sp^2 carbon atoms C(21), C(31), and C(32). Although C(22)–C(21), C(22)–C(32), and C(22)–C(23) carbon–carbon bonds present usual lengths for σ C–C bonds, the sp^3 hybridization of C(22) appears very distorted [C(21)–C(22)–C(32) = 83.6 (1.0)°]. It is noteworthy that this organic skeleton may also be viewed as including a C(1)C(21)C(31)C(32)-substituted 1,3-butadiene fragment, the conjugated double bonds of which explain the planarity.

The σ-alkenyl group bound to the exo sulfur atom S(2) appears with usual features. The central C=C bond length is slightly longer [1.343 (17) Å] than the corresponding value in **6** [1.308 (5) Å].

While the three nitrile groups present a typical C–N bond length of ca. 1.13 (2) Å, the C–CN bond lengths are quite different and depend strongly on the hybridization of the carbon atom: 1.490 (18) Å for the [sp^3-C(22)]–CN bond; 1.407 (19) and 1.391 (18) Å for the [sp^2-C]–CN bonds from C(12) and C(32). These differences are clearly indicative of a delocalization of the π-electron system of the CN group when bound to a sp^2-carbon atom.

3. Molecular Orbital Analysis of the Reactivity of the Mo–η^2-CS_2 Complex. To summarize the behavior of the complexes L_4Fe–η^2-CS_2 and Cp_2Mo–η^2-CS_2 toward activated alkynes, we recall that only the metallacycle B is commonly formed by both species. The metal–carbene form A is not found in the reaction products of Cp_2Mo–η^2-CS_2, while a new type of metallacycle, C, is uniquely obtained from Cp_2Mo–η^2-CS_2 (Figure 1). Bearing in mind the bonding features of L_4M–η^2-CS_2 systems,[6,7] we examine the orbital interaction diagram for Cp_2Mo–η^2-CS_2. At the left side of Figure 9 there is a set of Cp_2Mo fragment orbitals[30] and, at the right side, the bent CS_2 orbital.[31] For convenience, orbitals of both fragments are labeled with respect to C_{2v} symmetry, though it should be remembered that the resultant molecule belongs to a lower symmetry C_s point group.

As already mentioned, a d^4 Cp_2M fragment is isolobal with a d^8 L_4M fragment, as both have a HOMO/LUMO pair of π and σ character. A major difference in the frontier zone is that the Cp_2Mo fragment has an *extra* orbital, $1a_1$, not carried by a d^8 L_4M. This nonbonding orbital, drawn in I, is a result of mixing $x^2 - y^2$ and z^2 on

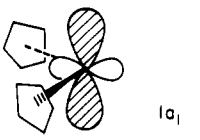

I

Mo. Notice that although the symmetry would allow some mixing between $1a_1$ and $2a_1$ levels, the former remains essentially nonbonding as its large lobes are laterally displaced. Ultimately, the picture of the interaction with CS_2 resembles, to a great extent, that of a d^8 L_4M–η^2-CS_2 species: The Mo *xy* orbital (b_2) interacts strongly with CS_2

(30) Albright, T. A.; Burdett, J. K.; Whangbo, M.-H. *Orbital Interactions in Chemistry*; John Wiley: New York, 1985; pp 394–401.

(31) Gimarc, B. M. *Molecular Structure and Bonding*; Academic Press: New York, 1979.

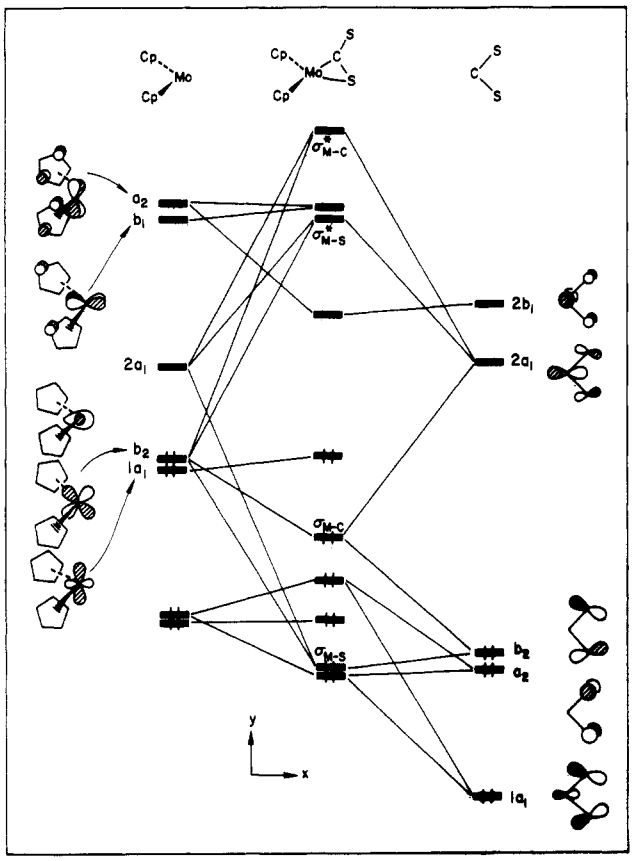

Figure 9. The orbital interaction diagram for $Cp_2Mo-\eta^2-CS_2$. At left are the fragment orbitals of Cp_2Mo and at right, those of the bent CS_2 species.

$\pi_\sigma^*(2a_1)$ to form a Mo–C σ bond. The Mo–S bonding comes largely from metal $2a_1$ (z^2 plus some sp_x) and CS_2 $n_\sigma(b_2)$ interaction.

As we did previously for the Fe model,[7] we follow the possible pathways to approach either the metallacyclic ring B and the 1,3-dithiol-2-ylidene complex A. The corresponding Walsh diagrams are very similar to those of iron, except for the presence of the extra nonbonding $1a_1$ level, which stays unaffected during both processes. We also find that the energy barriers for the reaction are again comparable for the two mechanisms. These are 1.3 and 1.4 eV, respectively. Here, however, the total energy of the carbene structure A is much higher than that of the isomer B, the ΔE being 1.0 eV (ΔE is only 0.3 eV for the Fe system). As shown in II, structure A is even destabilized by 0.5 eV with respect to the starting point, i.e. a $Cp_2Mo-\eta^2-(CS_2)(C_2H_2)$ species characterized by the *dangling* alkyne.

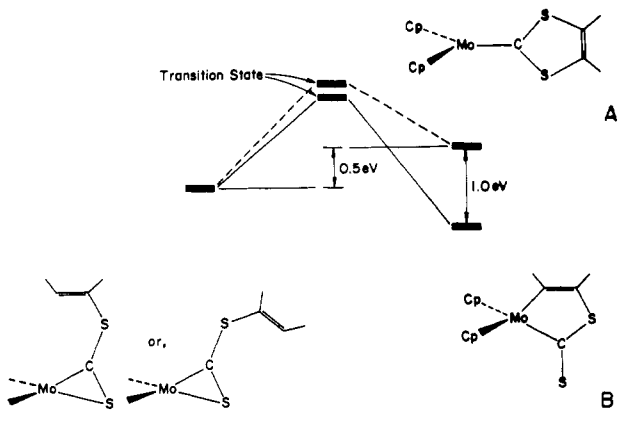

II

What makes the Mo metal–carbene structure so unstable? Two factors can be considered. First, let us redraw in **III** the most important M–C σ-bonding interactions for both Fe and Mo complexes. It was found for the former

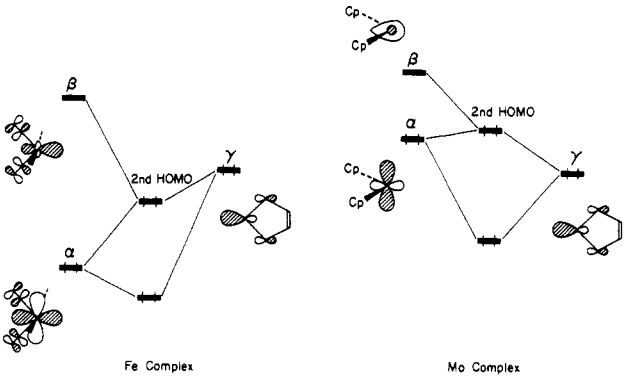

III

that M–C σ bonding comes mainly from the interaction of metal $z^2 + sp_x$ (labeled β) and CS_2 π_σ^* (labeled γ), with some contribution from a second metal orbital (labeled α). In the case of molybdenum, α is the nonbonding orbital $1a_1$, which lies in the frontier region. The relative energy difference of α and γ in the two systems is remarkable. In addition, β carries a percentage of sp_x character larger for the Fe than for the Mo fragment. As an indication, the calculated overlap population between β and γ is 0.40 for the former but only 0.35 for the latter. From these considerations one concludes that σ_{m-c}, the second HOMO in Figure 9, is stabilized more in the iron–carbene complex than in the Mo analogue. Also, it is clear that the compounds in question behave somewhat differently from the typical metal–carbene complexes. In fact, the γ orbital of the $(CS_2)(C_2H_2)$ ring resembles very much the high lying π_σ^* level of CS_2 and is even destabilized with respect to it. At the extended Hückel level the γ orbital is calculated ca. 2.2 eV higher than the corresponding carbon σ orbital in a pure CH_2 fragment.

Secondly, let us take a look at the difference between the two Fe and Mo systems when forming a metallacycle of type B. The features of the interaction diagram for latter, not reported in full, are similar to those already presented for the iron model.[7] One relevant comparison is made in IV. The metal d_π orbital, α, shown at left (Fe),

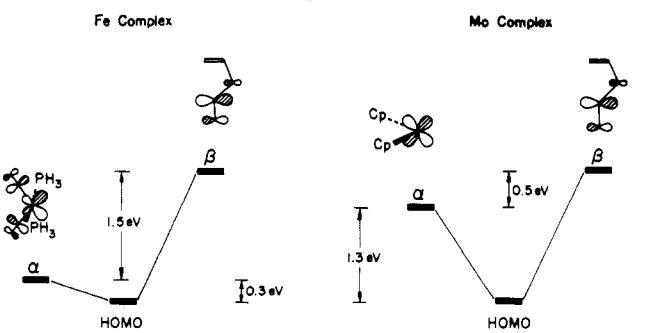

IV

is much lower for Fe than for the one shown at right (Mo), due both to the fact that 3d orbitals are lower for Fe than for Mo (the energy values used in our calculations are −12.7 and −10.5 eV, respectively) and that the back-donation to CO in Fe complex stabilizes α.

As a result, the α–β interaction, forming the HOMO, is stronger for the $Mo-CS_2$ complex because of the smaller energy gap. A great stabilization of the HOMO, and of the whole system as well, ensues. An important point to be made is that on account of second-order perturbation

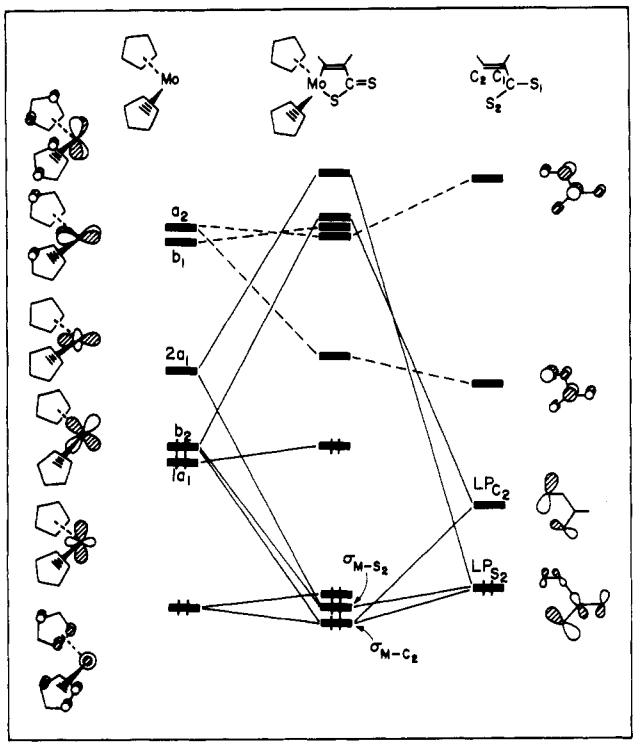

Figure 10. Schematic diagram illustrating the orbital interactions for the formation of the metallacycle C. The $(CS_2)(C_2R_2)$ fragment orbitals are given on the right side. The Cp_2Mo orbitals are sketched on the left and are labeled according to C_{2v} symmetry.

theory arguments (α lower than β)[32] the M–C interaction can still be regarded as a back-donation from the metal, with no oxidation state variation. The effects displayed in III and IV are summarized in V and schematize the relative stabilities of metal–carbene (A) versus metallacycle (B) species.

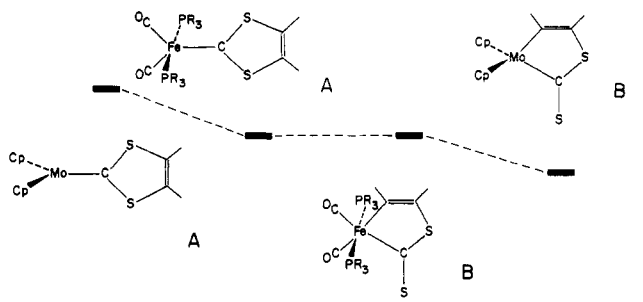

V

To form a new metallacyclic ring structure, C, one breaks a Mo–C bond instead of a Mo–S bond and forms a new $C–C_{acetylene}$ linkage in place of a $S–C_{acetylene}$ one. The fragment orbital analysis in Figure 10 clearly indicates the origin of the bonds in C. The lone pair on the sulfur atom S_2 is donated to the metal $2a_1$ orbital, giving rise to a Mo–S bond. The $b_2(3d_{xy})$ on metal finds a match with the orbital indicated as LP_{C_2} and forms a strong Mo–C_2 σ bond.

Notice that now the metal b_2 level lies at higher energy than the orbital localized on the C_2 atom. In such a case the two electrons used to form the Mo–C_2 bond can be formally assigned to the carbon atom and consequently the metal is to be considered oxidized. With such a picture of the levels for the final product, one can attempt a description of the correlations in the Walsh diagram leading to it.

(32) Hoffmann, R. *Acc. Chem. Res.* **1971**, *4*, 1.

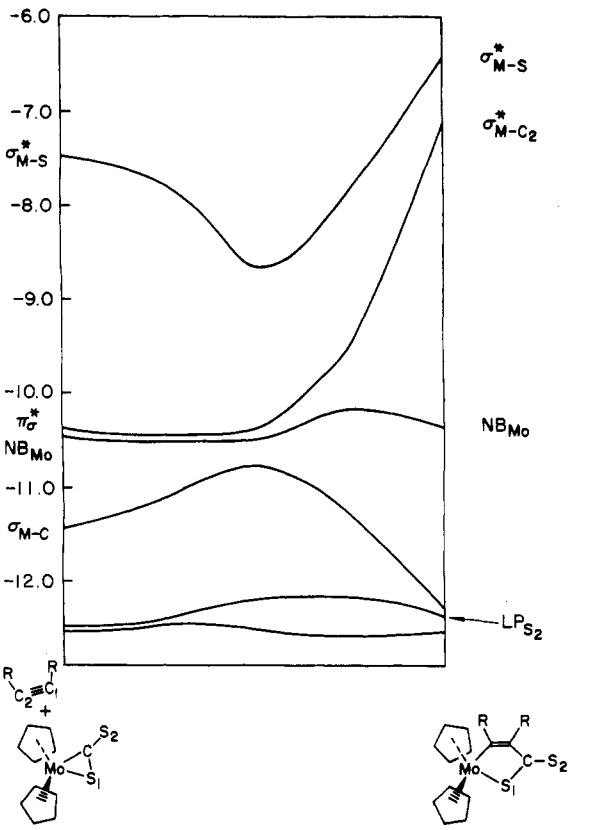

Figure 11. Walsh diagram of the process shown in VI. The orbital labeled NB_{Mo} is the metal nonbonding orbital $2a_1$. The geometrical variables associated with the process are listed in section 7 the Experimental Section.

We propose mechanism VI for the reaction which, starting from η^2 coordination, implies cleavage of the Mo–C bond, followed by formation of new C–C and Mo–C linkages. The cleavage of the original M–C bond does not

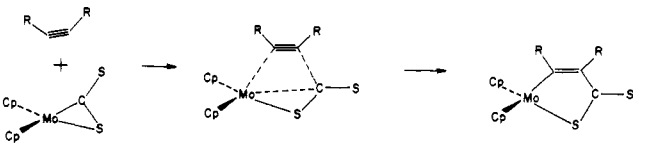

VI

necessarily imply a great loss of energy. This result was computationally found for a class of $L_3M–\eta^2$-CS_2 complexes for which the interconversion of the bent coordinated heteroallene to linearity costs less than 10 kcal mol^{-1}.[33] This is not suprising, in view of the nature of such a M–C bond, actually a back-donation from metal to carbon. More explicitly the carbon atom in η^2-coordination cannot be regarded as a two-electron donor and the energetics of the M–C bond are not comparable with that, say, of M–C_{alkyl} bonds.[34]

Figure 11 shows the correlation diagram for the process VI. At the left side three frontier orbitals are packed within a range of ca. 1 eV in energy. These are, in ascending order, the well-known σ_{M-C} bonding orbital, the nonbonding metal $2a_1$ orbital of $Cp_2Mo–\eta^2$-CS_2 (see Figure 9), and finally the acetylene π_σ* level. At large distance from the metal the latter π_σ* level is definitely empty. Increasing bending of the H–C–C angles in acetylene ($\approx$ 130–120°) stabilizes the level in question, more or less down to the same energy as $2a_1$. For us it is not so im-

(33) Mealli, C.; Hoffmann, R.; Stockis, R. *Inorg. Chem.* **1984**, *23*, 56.
(34) Ziegler, T.; Tschinke, V.; Becke, A. *J. Am. Chem. Soc.* **1987**, *109*, 1351.

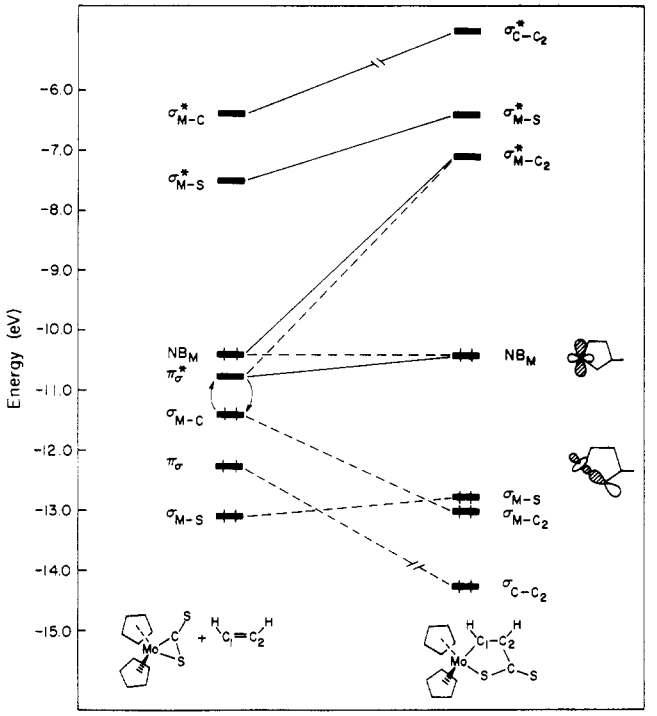

Figure 12. Orbital correlation scheme for the metalla ring structure C. The avoided crossings are represented by dashed lines.

portant to know the precise position of π_σ^* at the initial point of the Walsh diagram but rather to follow its mixing with the other levels along the pathway. Initially σ_{M-C} rises because of the loss of M–C bonding. The other two levels remain substantially unaltered, but halfway along the reaction path all of them can intermix. In the second part of the diagram, while $2a_1$ comes out almost unperturbed, the other two levels diverge. One of them acquires Mo–$C_{acetylene}$ bonding character, and the other one, d_{xy}, rises sharply as it becomes involved in an antibonding interaction with a combination of sulfur and C_2 σ orbitals. The situation is conveniently schematized in Figure 12.

The point made clear is that the C_2 (acetylene carbon) character, originally localized in π_σ^*, is transferred to the bonding σ_{M-C_2} MO, deep in energy. Ultimately it can be assumed that along the pathway two electrons have been formally transferred from the metal to the C_2 carbon atom. The metal oxidation and the consequent attainment of a formal 2– charge by the CS_2/C_2R_2 coupling product is a feature unique for the reaction leading to complex C. Computationally, we calculate less than 1 eV barrier for the process. Interestingly, a similar coupling reaction carried out starting from $(PR_3)_2(CO)_2Fe$–η^2-CS_2 encounters a barrier about twice as large (ca. 1.8 eV). A rationale for such a difference is as follows. The σ_{M-C} bond of the Fe–η^2-CS_2 fragment (HOMO) is allowed to rise high in energy (we calculate 0.7 eV) before the mixing with the descending acetylene π_σ^* level (LUMO) can occur. In addition some other lower levels are destabilized. In the molybdenum species the destabilization of the equivalent σ_{M-C} level (second HOMO) is not so high, due to the presence of the level $2a_1$ (HOMO), which acts as a buffer preventing σ_{M-C} from rising too much in energy. In other words, the important and dramatic effect of mixing and switching character engages directly the HOMO/LUMO levels in the iron system but only the second HOMO/LUMO levels in the molybdenum one, where the HOMO plays a mitigating role. Notice that in the iron system the equivalent of the $1a_1$ level, I, is a member of the t_{2g} set

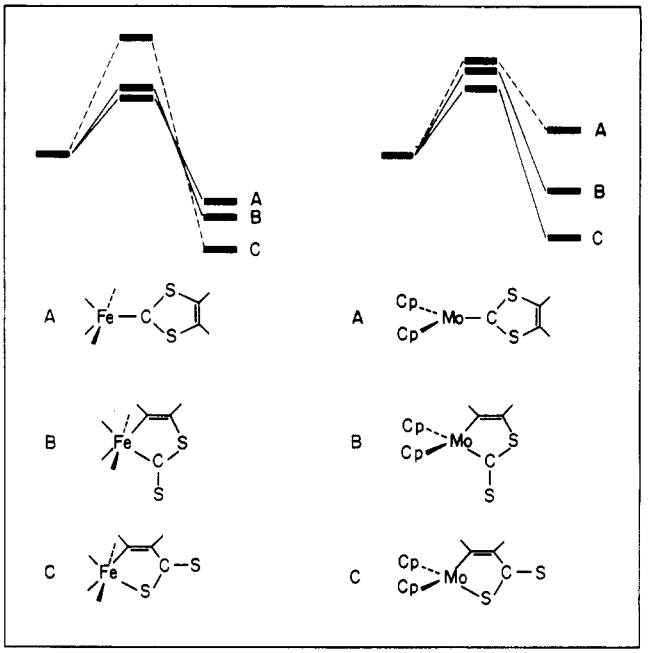

Figure 13. Relative stability of the three different coupling products obtainable from an alkyne molecule and $[L_4Fe(\eta^2\text{-}CS_2)]$ (a) or $[Cp_2Mo(\eta^2\text{-}CS_2)]$ (b).

which starts lower than the σ_{M-C} level even in the L_4Fe–η^2-CS_2 complex and never crosses with it.

Qualitatively, we believe that formation of the 2:1 (η^2-CS_2)–alkyne complexes **5** and **6** from the type B 1:1 adducts (**2** and **3**) may proceed through the mechanism shown in VII. First, an electrophilic attack of the exo

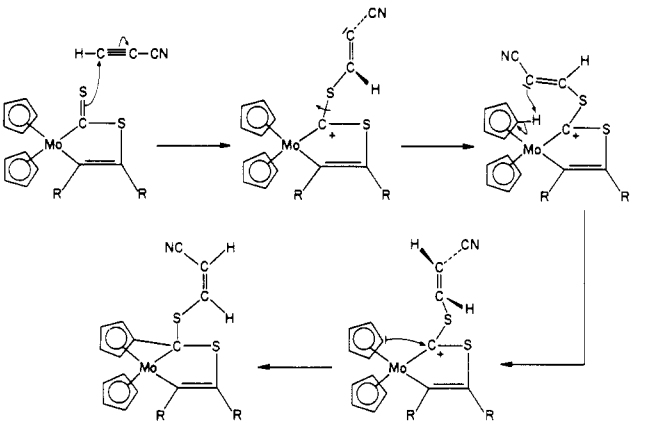

VII

sulfur atom by the acetylenic carbon bound to H seems to be likely. In the resulting intermediate species with a dangling alkyne, the exoCS_2 carbon atom presents strong electrophilic character while the α-carbon atom of the alkyne relative to the CN group has a lone pair. By rotation of the dangling alkyne, this lone pair may approach and attack the C_5H_4 ligand, with cleavage of a CH bond and migration of a proton onto the vinylic fragment. Formation of the carbon–carbon bond between the C_5H_5 ligand and the exoCS_2 carbon atom then completes building of the molecule.

Figure 13 presents a summary of the relative stability of the three different coupling products obtainable from a η^2-coordinated CS_2 molecule and one activated acetylene molecule, starting from both L_4M–η^2-CS_2 and Cp_2Mo–η^2-CS_2 precursors. Interestingly, there is at least one good reason to justify the missing member in each series. Thus, the 1,3-dithiol-2-ylidene adduct is not obtainable with molybdenum, due to a large energy destabilization of the

adduct itself. Conversely, for iron, a metallacycle of type C finds a large energy barrier along the pathway to its formation due to the destabilization of some filled orbitals. Ultimately, this is due to the difficulty of transferring electrons from the metal to the acetylene carbon atom.

Acknowledgment. We thank MRT for financial support of the form of scholarship (F.C.) and the CNRS for partial financial support. We are indebted to Dr. Brevard for recording NMR spectra on a Bruker AM 400 spectrometer and stimulating discussions.

We are grateful to NATO for its generous support of this research through Grant No. 200.81, which made this collaboration possible. J.L. would like to express her thanks to the members of ISSECC for their hospitality during her stay in Florence. We thank Joyce Barrows for the production of this manuscript and Jane Jorgensen and Elisabeth Fields for the drawings.

Registry No. 1, 112803-32-4; 2, 119382-09-1; 3, 119382-10-4; 4, 119382-11-5; 5, 119382-13-7; 6, 119434-98-9; 7, 119382-14-8; 8, 121056-08-4; 9, 5512-84-5; dmad, 762-42-5; $CF_3C{\equiv}CCF_3$, 692-50-2; $HC{\equiv}CCN$, 1070-71-9.

Supplementary Material Available: Tables of anisotropic thermal parameters for 2, 4, 6, and 7 and hydrogen atom coordinates for 4, 6, and 7 (7 pages); listings of structure factors for 2, 4, 6, and 7 (44 pages). Ordering information is given on any current masthead page.

Synthesis and Properties of Some New (η^6-Arene)cobalt Complexes

Helmut Bönnemann,* Richard Goddard, Joachim Grub, Richard Mynott, Eleonore Raabe, and Stefan Wendel

Max-Planck-Institut für Kohlenforschung, Kaiser-Wilhelm-Platz 1, D-4330 Mülheim a. d. Ruhr, Federal Republic of Germany

Received December 15, 1988

The preparation of several new types of (η^6-arene)cobalt complexes is described. (η^3-Cyclooctenyl)(η^2,η^2-cyclooctadiene)cobalt (**1**) reacts with H_2 in the presence of arenes and N bases such as piperidine to form (η^6-arene)(η^1,η^2-cyclooctenyl)cobalt complexes (**2**). The structure of the 1-η^1,4,5-η^2-cyclooctenyl ligand was determined by 2D NMR techniques. Complexes **2** react with $HBF_4{\cdot}Et_2O$ in the presence of dienes to give (η^6-arene)(diene)cobalt tetrafluoroborates (**5**, **6**, **8**, **10**), which in turn react with $NaBEt_3H$ to afford (η^6-arene)(η^3-allyl)cobalt complexes. When the latter are treated with $HBF_4{\cdot}Et_2O$ in the presence of dienes, then (η^6-arene)(diene)cobalt tetrafluoroborates are re-formed. (η^6-Arene)(butadiene)cobalt tetrafluoroborates can be prepared by treating (5-methylheptadienyl)(η^4-butadiene)cobalt with $HBF_4{\cdot}Et_2O$ in the presence of arenes. The reaction of **1** with $HBF_4{\cdot}Et_2O$ and arene results in the synthesis of (η^6-arene)(η^1,η^3-cyclooctenediyl)cobalt(III) tetrafluoroborate complexes (**18**). The NMR evidence for this structure is discussed. The arene ligand in **18** is easily displaced by acetonitrile to give (η^1,η^3-cyclooctenediyl)tris(acetonitrile)cobalt tetrafluoroborate (**21**), which is a versatile compound for the synthesis of neutral cobalt complexes with η^1,η^3-cyclooctenediyl ligands. The crystal structures of (η^5-cyclopentadienyl)(η^1,η^3-cyclooctenediyl)cobalt (**22**) and (acetylacetonato)(η^1,η^3-cyclooctenediyl)cobalt (**23**) were confirmed by X-ray diffraction techniques. Crystals of **22** are tetragonal, space group $P\bar{4}$, with $a = b =$ 16.583 (2) Å, c = 7.995 (1) Å, and $Z = 8$; $R = 0.031$ for 2525 unique observed reflections. Crystals of **23** are triclinic, space group $P\bar{1}$, with a = 8.4165 (8) Å, b = 8.9539 (9) Å, c = 9.3770 (5) Å, α = 72.588 (5)°, β = 72.224 (5)°, γ = 70.521 (8)°, and $Z = 2$; $R = 0.033$ for 3160 unique observed reflections. Both complexes are monomeric and contain similar $C_8H_{12}Co$ fragments.

Introduction

In the past 30 years a number of neutral and cationic η^6-arene complexes of cobalt[1] have been synthesized in which the arene is benzene, an alkylated benzene, or an annelated arene. However, only a few examples of arene–cobalt complexes are known where the arene ligands bear functional groups.[2] In this paper we wish to report some novel cationic and neutral arene–cobalt complexes with arenes and functionized arenes. We also report some compounds containing ligands that are η^1,η^2-, η^3-, or η^1,η^3-bound to cobalt, some of which are of types previously unknown for this metal.

Results and Discussion

1. (η^6-Arene)(η^1,η^2-cyclooctenyl)cobalt Complexes (2). The reaction of (η^3-cyclooctenyl)(η^2,η^2-cyclooctadiene-1,5)cobalt (**1**)[3,4] with H_2 at room temperature in benzene solution leads to hydrogenation and decomposition of **1** to metallic cobalt, cyclooctane, and cyclohexane (eq 1). However, when basic auxiliary ligands (for example, an amine such as piperidine) are added, the formation of metallic cobalt is suppressed almost completely and the

(1) (a) Silverhorn, W. E. *Adv. Organometal. Chem.* **1975**, *13*, 47. (b) Gastinger, R. G.; Klabunde, K. J. *Transition Met. Chem. (Weinheim, Ger.)* **1979**, *4*, 1. (c) Kemmitt, R. D. W.; Russel, D. R. In *Comprehensive Organometallic Chemistry*; Wilkinson, G., Stone, F. G. A., Abel, E. W., Eds.; Pergamon Press: New York, 1982; Vol. 5. (d) Geiger, W. E.; Edwin, J. *Organometallics* **1984**, *3*, 1910. (e) Jonas, K. *Angew. Chem., Int. Ed. Engl.* **1985**, *24*, 295. (f) Bönnemann, H. *Angew. Chem. Int. Ed. Engl.* **1985**, *24*, 248.

(2) (a) Efraty, A.; Maitlis, P. M. *J. Am. Chem. Soc.* **1967**, *89*, 3744. (b) Fairhurst, G.; White, C. *J. Chem. Soc., Dalton Trans.* **1979**, 1531.

(3) Otsuka, S.; Rossi, M. *J. Chem. Soc. A* **1968**, 2630.

(4) Grard, Ch. Dissertation, Ruhr-Universität Bochum, 1967.

0276-7333/89/2308-1941$01.50/0